J. Fluid Mech. (2002), *vol.* 459, *pp.* 139–166.
DOI: 10.1017/S0022112002007905 Printed in the United Kingdom

A new approach to modelling near-wall turbulence energy and stress dissipation

By S. JAKIRLIĆ[1] AND K. HANJALIĆ[2]

[1]Institute of Fluid Mechanics and Aerodynamics, Darmstadt University of Technology, Petersenstr. 30, 64287 Darmstadt, Germany

[2]Faculty of Applied Physics, Delft University of Technology, Lorentzweg 1, 2628 CJ Delft, The Netherlands

(Received 1 August 2000 and in revised form 29 October 2001)

A new model for the transport equation for the turbulence energy dissipation rate ε and for the anisotropy of the dissipation rate tensor ε_{ij}, consistent with the near-wall limits, is derived following the term-by-term approach and using results of direct numerical simulations (DNS) for several generic wall-bounded flows. Based on the two-point velocity covariance analysis of Jovanović, Ye & Durst (1995) and reinterpretation of the viscous term, the transport equation is derived in terms of the 'homogeneous' part ε^h of the energy dissipation rate. The algebraic expression for the components of ε_{ij} was then reformulated in terms of ε^h, which makes it possible to satisfy the exact wall limits without using any wall-configuration parameters. Each term in the new equation is modelled separately using DNS information. The rational vorticity transport theory of Bernard (1990) was used to close the mean curvature term appearing in the dissipation equation. *A priori* evaluation of ε_{ij}, as well as solving the new dissipation equation as a whole using DNS data for quantities other than ε_{ij}, for flows in a pipe, plane channel, constant-pressure boundary layer, behind a backward-facing step and in an axially rotating pipe, all show good near-wall behaviour of all terms. Computations of the same flows with the full model in conjunction with the low-Reynolds number transport equation for $\overline{u_iu_j}$, using ε^h instead of ε, agree well with the direct numerical simulations.

1. Introduction

The transport equation for the turbulence energy dissipation rate

$$\varepsilon = \nu \overline{\frac{\partial u_i}{\partial x_k} \frac{\partial u_i}{\partial x_k}}$$

has been widely used to close single-point $k-\varepsilon$ eddy-viscosity and second-moment (Reynolds stress transport) models.† Motivation for modelling and solving an equation for ε comes from the fact that ε appears as the sole viscous sink in the transport equation for the turbulence kinetic energy, hence no need for modelling. Furthermore, the classic similarity theory (though valid only for equilibrium turbulence) suggests ε

† Although ε does not represent the true dissipation rate $\overline{\tau_{ij}s_{ij}} = \frac{1}{2}\nu\overline{(\partial u_i/\partial x_j + \partial u_j/\partial x_i)^2}$, where τ_{ij} is the fluctuating viscous stress and s_{ij} the fluctuating strain rate, in the viscous and inner turbulent region close to a smooth solid surface (and everywhere else) the difference term $\nu(\partial^2\overline{u_iu_j}/\partial x_i\partial x_j)$, representing an 'extra' viscous diffusion was found from DNS data for a channel flow to be less than 2% of the total dissipation, and hence, negligible (Bradshaw & Perot 1993).

as a convenient parameter to define characteristic turbulence time or length scales in conjunction with the turbulence energy k, or with components of the turbulent stress tensor $\overline{u_i u_j}$.

Two major concerns have been frequently expressed regarding the practice of using ε and its transport equation for closure purposes. First, it has been argued that the characteristic turbulence scale in single-point closure should be expressed in terms of the spectral energy transfer rate, which equals the energy dissipation rate only in the case of spectral equilibrium. Second, the model equation for ε has been formally linked to its exact antecedent, although there is no physical correspondence among various terms, except for the rate of change and molecular diffusion. These are the only terms which can be treated in the exact form, and which ensure that the equation retains the standard conservative form. The inherent inability of single-point closure to account for any spectral dynamics places a serious limitation on overcoming the first concern. However, the standard model equation for ε, derived heuristically (with turbulence energy production providing the main and only source term) and tuned in some simple equilibrium flows, has often been interpreted more as an empirical equation for the spectral transfer, than for true ε.

Recent direct numerical simulations (DNS) provided information about individual terms in the ε equation, so that the model for each term can be verified. Based on term-by-term scrutiny, the model ε equation should reflect better the true dynamics of the exact ε equation, as demonstrated in this paper. This, in turn, should diminish the above mentioned spectral transfer–dissipation rate inconsistency since all unknown terms in all transport equations that constitute a model will be modelled with ε provided from the model equation that now mimics the exact dissipation equation. Of course, the prerequisite is that the term-by-term modelling satisfies not only simple equilibrium flows such as in a fully developed plane channel, but also more complex flows where spectral transfer may deviate from the dissipation rate.

The DNS of some simple flows showed that even at local energy equilibrium conditions the models for major interactions in the transport equation for ε do not adequately reflect the corresponding terms in the exact ε equation. This is particularly pronounced in low-Reynolds-number near-wall flow regions where the dynamics of dissipative correlation is strongly affected both by viscosity and by the non-viscous blocking effect of a solid wall. The success in reproducing ε reasonably well, even at low Reynolds numbers and near walls, is achieved by *ad hoc* tuning of the equation as a whole; this is, in fact, a procedure whose success depends on the compensation of errors made in the models for each term. The application of such models in non-equilibrium situations, different from those in which the models were calibrated, often leads to unsatisfactory results.

Various extensions of the ε equation have been proposed to account for extra strain effects, streamline curvature, rotation, buoyancy, as well as for differentiating the effects of rotational and irrotational strain, or for accounting for spectral non-equilibrium. While such extensions yielded improvements for some classes of flows, they failed in others. The lack of success in extending the modelled equation for ε has been the main reason for a persistent use of the rudimentary form (single source and sink terms) despite notable shortcomings proven over the years of extensive model validation.

Most of the activities in refining and extending the model ε equation have focused on the effects of viscosity and wall proximity. These modifications have been considered essential for predicting wall phenomena – friction and heat transfer in wall-bounded flows. These require integration of the modelled equations up to the

wall, instead of using standard (equilibrium) wall functions to bridge the near-wall viscous layer.

Bradshaw, Launder & Lumley (1991), showed that none of the available models could reproduce a behaviour of ε very close to the wall that would agree with the results of DNS. In fact most models predict the maximum value of ε to be away from the wall (at about $y^+ \approx 10$) whereas the DNS results indicate that ε reaches its maximum value at the wall. More recently several modifications have been suggested which remedied this deficiency (Nagano & Shimada 1993; Rodi & Mansour 1993; Kawamura & Kawashima 1995). Although based on scaling or some other theoretical arguments, most proposals end with compromising solutions to match the wall-limiting behaviour, mainly by virtue of one or more additional terms, which compensate for the model deficiency very close to the wall.

In second-moment (Reynolds-stress) closure models the problem becomes even more challenging because of a need to model each component of the dissipation rate tensor

$$\varepsilon_{ij} = 2\nu \overline{\frac{\partial u_i}{\partial x_k} \frac{\partial u_i}{\partial x_k}},$$

which represents the sink of turbulent stresses. While a transport equation for ε_{ij} can be derived and modelled (e.g. Durbin & Speziale 1991; Tagawa, Nagano & Tsuji 1991; Speziale & Gatski 1997; Oberlack 1997), such an equation is burdened by even greater uncertainties and a number of additional empirical coefficients which need to be determined. Because ε_{ij} is expected to approach an isotropic state ($\frac{2}{3}\varepsilon\delta_{ij}$) at high Reynolds numbers and at a sufficiently large distance from a solid wall or phase interface, solving six additional differential transport equations for ε_{ij} does not seem rational for practical computations. Besides, in view of the large uncertainties remaining in modelling other terms in the equations for turbulent stresses $\overline{u_i u_j}$, e.g. the pressure–strain correlation which acts as a major source or sink of individual stress components, such an effort at present does not seem worthwhile. An algebraic modelling of ε_{ij}, while solving the transport equation for its half trace ε, seems a more viable approach, provided improvement of the ε equation can be achieved, particularly in flows where ε_{ij} is strongly anisotropic.

In this paper we revisit the dissipation equation and present some results from a different approach appropriate to low-Reynolds-number near-wall flows. There are two aspects that distinguish the present approach from others. First, the derivation of the equation for ε is based on the transport equation for the two-point correlation (e.g. Jovanović, Ye & Durst 1995). Second, a *term-by-term* modelling of the individual terms in the dissipation equation is applied, combined with the algebraic relationship for ε_{ij} in term of ε, stress and dissipation tensor invariants and the turbulence Reynolds number Re_t.

The present interpretation provides a better reproduction of the DNS results on the basis of different interpretation of the viscous term in the stress equation, with the aid of the dynamic equation for the two-point velocity covariance. It is shown that the new equation for the 'homogeneous' dissipation rate:

$$\varepsilon^h = \varepsilon - \tfrac{1}{2}\nu \frac{\partial^2 k}{\partial x_l \partial x_l} \tag{1.1}$$

differs from the standard one only in the factor $1/2$ in the viscous diffusion term, which is important only very close to a solid wall. However, this new formulation offers several advantages.

2. The viscous term in $\overline{u_iu_j}$ equation

The exact transport equation for the turbulent stress tensor contains the viscous term which in the original derivation takes the form

$$\frac{\mathrm{D}\overline{u_iu_j}}{\mathrm{D}t} = -\left(\overline{u_iu_k}\frac{\partial U_j}{\partial x_k} + \overline{u_ju_k}\frac{\partial U_i}{\partial x_k}\right) - \frac{\partial \overline{u_iu_ju_k}}{\partial x_k} + \frac{1}{\rho}\left(\overline{u_i\frac{\partial p}{\partial x_j}} + \overline{u_j\frac{\partial p}{\partial x_i}}\right) + \underbrace{\nu\left(\overline{u_i\frac{\partial^2 u_j}{\partial x_k\partial x_k}} + \overline{u_j\frac{\partial^2 u_i}{\partial x_k\partial x_k}}\right)}_{V_{ij}}. \tag{2.1}$$

Our interest here lies with the viscous terms V_{ij}. It is customary to split the viscous term into two parts: one representing the viscous diffusion of the turbulent stress tensor $\overline{u_iu_j}$; the other, ε_{ij}, representing the viscous dissipation rate of $\overline{u_iu_j}$:

$$V_{ij} = \nu\frac{\partial^2\overline{u_iu_j}}{\partial x_k\partial x_k} - 2\nu\overline{\frac{\partial u_i}{\partial x_k}\frac{\partial u_j}{\partial x_k}} = \mathscr{D}^{\nu}_{ij} - \varepsilon_{ij}. \tag{2.2}$$

The first term, of course, requires no closure. Our interest is in the dissipation tensor. Modelling this term is the subject of the next section.

2.1. *Current modelling practice for* ε_{ij}

Most current models employ an algebraic relationship for the deviatoric components of the stress dissipation-rate tensor ε_{ij} in terms of the deviatoric of the stress tensor, $\overline{u_iu_j}$, which assumes direct proportionality between the anisotropy of the large-scale stress-bearing eddies, and the small-scale dissipative eddies, i.e.

$$e_{ij} = f_s\, a_{ij}, \tag{2.3}$$

where

$$e_{ij} = \frac{\varepsilon_{ij}}{\varepsilon} - \tfrac{2}{3}\delta_{ij}, \qquad a_{ij} = \frac{\overline{u_iu_j}}{k} - \tfrac{2}{3}\delta_{ij}, \tag{2.4}$$

and f_s is a blending function which relaxes the direct proportionality and ensures a smooth transition from small-scale anisotropic to isotropic turbulence. This assumption is not physically justified since the anisotropy of the stress-bearing motion, especially at higher Reynolds numbers, is not well correlated with usually more isotropic dissipative scales. Nevertheless, it has proved to be a reasonable approximation provided f_s is specified adequately. Equation (2.3) is often used in a more common form which gives the components of the dissipation rate directly in terms of the Reynolds stresses (Hanjalić & Launder 1976):

$$\varepsilon_{ij} = \varepsilon\left[(1-f_s)\tfrac{2}{3}\delta_{ij} + \frac{\overline{u_iu_j}}{k}f_s\right]. \tag{2.5}$$

The function f_s is expressed in terms of the turbulence Reynolds number $Re_t = k^2/(\nu\varepsilon)$, chosen such that $f_s \to 0$ as $Re_t \to \infty$, so that the dissipation tensor becomes isotropic: $\varepsilon_{ij} = \frac{2}{3}\varepsilon\delta_{ij}$. If the Reynolds number approaches zero, the function f_s takes the value of unity, ensuring the low-Re limit of (2.5), i.e. $\varepsilon_{ij} = (\overline{u_iu_j}/k)\varepsilon$. The common practice in the second-moment closure models is to solve the equation for ε and then to employ equation (2.5) to compute the components of ε_{ij}. Modelling the tensor ε_{ij} thus reduces to modelling the function f_s. Early models express f_s in terms of the turbulence Reynolds number $Re_t = k^2/\nu\varepsilon$, assuming that the anisotropy of ε_{ij} is

Authors	f_s	f_d	F
HL (1976)	$\dfrac{1}{1+0.1Re_t}$	0	0
KLY (1985)	$\exp\left(-\dfrac{Re_t}{40}\right)$	1	5/2
LT (1993)	$\exp(-20A^2)$	1	3/2
GK (1991)	$1-\sqrt{A}$	1	3/2
HJ (1993)	$1-\sqrt{A}E^2$	$\dfrac{1}{1+0.1Re_t}$	3/2

TABLE 1. Different proposals for the 'blending' function f_s in the model for ε_{ij}; HL – Hanjalić & Launder; KLY – Kebede, Launder & Younis; LT – Launder & Tselepidakis; GK – Gilbert & Kleiser; HJ – Hanjalić & Jakirlić.

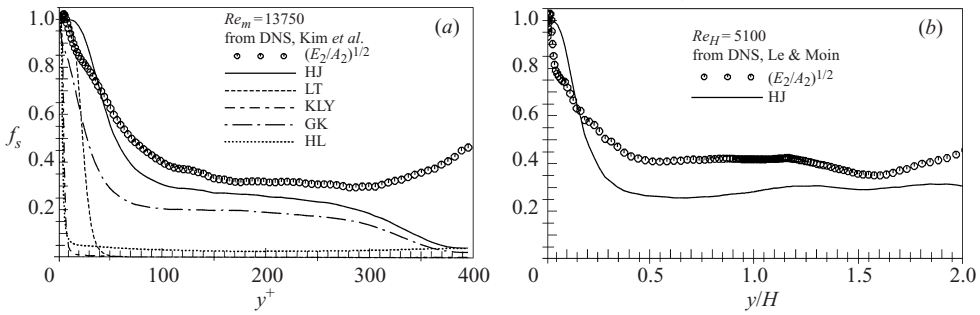

FIGURE 1. Profiles of the 'blending' function f_s in (*a*) fully developed channel flow and (*b*) reattaching region of the backward-facing step flow. For key to initials, see table 1 caption.

solely a consequence of viscous effects. The DNS revealed that the anisotropy in ε_{ij} in wall-bounded flows extends far beyond the viscous near-wall region (e.g. Mansour, Kim & Moin 1988; Durbin & Speziale 1991) and is due to non-viscous wall blocking and eddy flattening effects.

Subsequently, several authors expressed f_s in terms of second or third stress invariants $A_2 = a_{ij}a_{ji}$ and $A_3 = a_{ij}a_{jk}a_{ki}$, or the 'flatness' parameter $A = 1-9/8(A_2-A_3)$ (Gilbert & Kleiser 1991; Launder & Tselepidakis 1993). Lee & Reynolds (1987) suggested that small-scale anisotropy can be characterized by the anisotropy of the vorticity correlation, which can be linked to ε_{ij}. Following the argument that strong anisotropy and the eddy flattening effect by a solid wall are felt by the small-scale dissipative motion even if the Reynolds number has a relatively high value (Durbin & Speziale 1991), Hanjalić & Jakirlić (1993) introduced the flatness parameter of the small-scale dissipative motion, $E = 1-\frac{9}{8}(E_2-E_3)$, where $E_2 = e_{ij}e_{ji}$ and $E_3 = e_{ij}e_{jk}e_{ki}$ are the second and third invariants of the anisotropy of ε_{ij}. The proposed function f_s involves both E and A, i.e. $f_s = 1-\sqrt{A}E^2$. *A priori* validation against DNS results for a plane channel, using $f_s = \sqrt{E_2/A_2}$ as a reference target (that follows from equation (2.3)), shows satisfactory results. Table 1 shows several propositions, which are compared with $\sqrt{E_2/A_2}$ in figure 1. Other algebraic interpolations have also been proposed for ε_{ij}; e.g. Hallbäck, Groth & Johansson (1990) used the tensorial

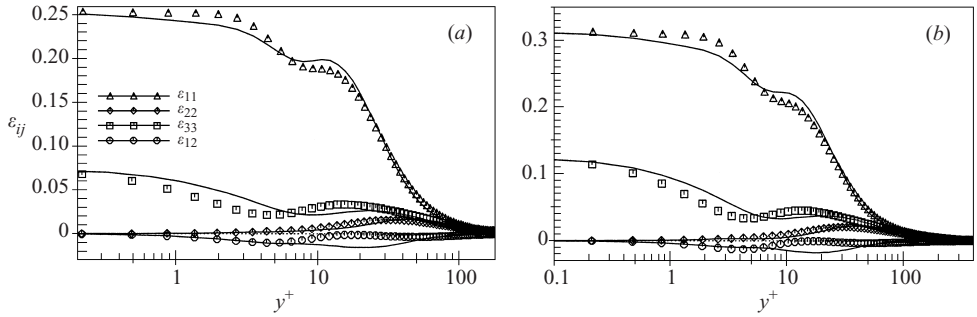

FIGURE 2. Components of ε_{ij} in fully developed channel flows at two bulk Reynolds numbers: (*a*) $Re_m = 5600$ and (*b*) $Re_m = 13\,750$. Symbols: DNS, Kim *et al.*; lines: HJ ε_{ij} model, equations (2.6)–(2.8).

expansion up to the quadratic term in terms of stress anisotropy a_{ij}. This expression was derived for homogeneous flows and compares poorly with DNS data for a channel flow (Jakirlić 1997).

A major difficulty with algebraic interpolation schemes in the form of equation (2.5) or similar is that they do not satisfy the near-wall limits for components ε_{12} and ε_{22}. In order to overcome this shortcoming, several modifications have been proposed. Launder & Reynolds (1983) proposed modifications involving the unit normal vectors, by which they distingushed wall limits for different components of ε_{ij}. However, their correction expression extended too far away from the wall into the region where ε seems to follow closely the $(\overline{u_i u_j}/k)\varepsilon$ pattern, to reduce gradually to the isotropic expression $\frac{2}{3}\varepsilon\delta_{ij}$. In order to remedy this deficiency, Hanjalić & Jakirlić (1993) modified the expression of Launder & Reynolds (1983) by introducing another function in terms of turbulence Reynolds number. The resulting expression is

$$\varepsilon_{ij} = (1 - f_s)\tfrac{2}{3}\delta_{ij}\varepsilon + f_s\varepsilon^*_{ij}, \tag{2.6}$$

where

$$\varepsilon^*_{ij} = \frac{\varepsilon}{k}\frac{\overline{u_i u_j} + (\overline{u_i u_k}n_j n_k + \overline{u_j u_k}n_i n_k + \overline{u_k u_l}n_k n_l n_i n_j)f_d}{1 + F(\overline{u_p u_q}/k)\, n_p n_q f_d}, \tag{2.7}$$

where

$$f_s = 1 - \sqrt{A}E^2, \quad f_d = (1 + 0.1Re_t)^{-1}, \quad n_p = (0,1,0), \quad F = \tfrac{3}{2}. \tag{2.8}$$

A priori testing by feeding in the DNS data for $\overline{u_i u_j}$ and ε in equations (2.6) to (2.8) gave good agreement with DNS results for all diagonal components of ε_{ij} for turbulent flow in a plane channel, as shown in figure 2 for two Reynolds numbers.

The agreement for the off-diagonal component, ε_{12}, is less satisfactory, though the discrepancy is hardly visible in the figures because in the viscous wall region this component is much smaller than the diagonal ones, and a unique scale was used for all components.

Of course, the real quality of predictions, when using the complete model, depends on the ability to predict accurately the energy dissipation rate ε and the stress tensor $\overline{u_i u_j}$ from the transport equations. It should also be noted that, despite success, the use of normal unit vectors in (2.7) is not very convenient for flows with complex geometries. Recently, Craft & Launder (1996) proposed an algebraic expression in which, instead of wall-normal unit vectors, the wall orientation and its configuration were accounted for by gradients of the turbulence kinetic energy and stress-flatness invariant parameter A, defined above. Excellent reproduction of the DNS data for

all components of ε_{ij} was reported for free-surface flow, shear-free wall and plane Couette flow. No results were published for separating or rotating flows. However, their expression is rather complex and the model for ε_{ij} is a part of a complex nonlinear second-moment closure.

We propose here an alternative route which ensures a better term-by-term reproduction and eliminates to a great extent the shortcomings mentioned above.

2.2. *Two-point results for* ε_{ij}

The transport equation for the two-point correlation (Jovanović *et al.* 1995) highlights the terms of interest as

$$\frac{\mathrm{D}\overline{(u_i)_A(u_j)_B}}{\mathrm{D}t} = \cdots + \underbrace{\nu\left[\overline{(u_i)_A\left(\frac{\partial^2 u_j}{\partial x_k \partial x_k}\right)_B} + \overline{(u_j)_B\left(\frac{\partial^2 u_i}{\partial x_k \partial x_k}\right)_A}\right]}_{V_{i,j}^{AB}} = \cdots + V_{i,j}^{AB}. \tag{2.9}$$

Introducing the local coordinate system with the origin at the midpoint between A and B and noting that $\xi_k = x_k^B - x_k^A$ and $x_k^{AB} = \frac{1}{2}(x_k^A + x_k^B)$, the viscous term $V_{i,j}^{AB}$ can be written in the following form for the general case of non-isotropic, non-homogeneous turbulence:

$$V_{i,j}^{AB} = \tfrac{1}{2}\nu\left(\frac{\partial^2}{\partial x_k \partial x_k}\right)_{AB}\overline{(u_i)_A(u_j)_B} + 2\nu\frac{\partial^2}{\partial \xi_l \partial \xi_l}\overline{(u_i)_A(u_j)_B}. \tag{2.10}$$

In homogeneous turbulence all derivatives with respect to $(x_k)_{AB}$ vanish and, for $A \to B$, $V_{i,j}^{AB} \to V_{ij}$ represents the dissipation in a homogeneous flow, ε^h:

$$V_{i,j}^{AB} \to V_{ij} = \left[2\nu\frac{\partial^2}{\partial \xi_l \partial \xi_l}\overline{(u_i)_A(u_j)_B}\right]_{\xi=0} = -\varepsilon_{ij}^h. \tag{2.11}$$

In inhomogeneous turbulence, for $A \to B$:

$$V_{i,j}^{AB} \to V_{ij} = \tfrac{1}{2}\nu\frac{\partial^2 \overline{u_i u_j}}{\partial x_k \partial x_k} - \varepsilon_{ij}^h = \tfrac{1}{2}\mathscr{D}_{ij}^{\nu} - \varepsilon_{ij}^h. \tag{2.12}$$

Comparison with the single-point derivation, equation (2.2), yields

$$\varepsilon_{ij} = \varepsilon_{ij}^h + \tfrac{1}{2}\mathscr{D}_{ij}^{\nu}. \tag{2.13}$$

The dissipation tensor has contributions due to the inhomogeneity of the flow that are usually treated as diffusive transport. Clearly, no algebraic interpolation for the ε_{ij} can account for the dissipation due to gradients of the Reynolds stresses.

2.3. *Modelling implications*

In view of the deficiency of the algebraic interpolation formula for ε_{ij} discussed above, it is clear that equation (2.5) can only be used for the *homogeneous* part of the dissipation rate tensor,

$$\varepsilon_{ij}^h = (1 - f_s)\tfrac{2}{3}\delta_{ij}\varepsilon^h + f_s\frac{\overline{u_i u_j}}{k}\varepsilon^h. \tag{2.14}$$

The components of the full dissipation-rate tensor can now be obtained from equation (2.13) where $\mathscr{D}_{ij}^{\nu}$ is the viscous diffusion of the corresponding stress component, computed from the solution of the stress transport equations.

An advantage of using this approach is immediately apparent: the expression for ε_{ij} satisfies exactly the wall limits of each normalized dissipation component

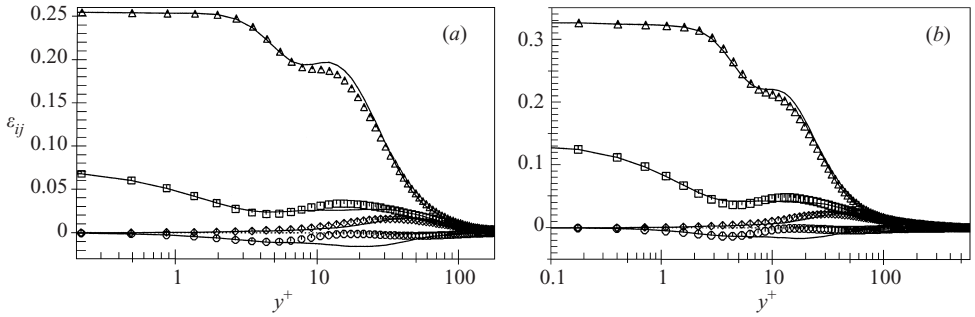

FIGURE 3. Components of ε_{ij} in fully developed channel flows at two bulk Reynolds numbers: (*a*) $Re_m = 5600$ and (*b*) $Re_m = 22\,000$. Lines: equations (2.13–2.14); symbols as figure 2.

$(\varepsilon_{ij}/\varepsilon)(k/\overline{u_i u_j})$, (no sum on repeated indices) which is 1 for $i = j = 1$, $i = j = 3$ and $i = 1$, $j = 3$, and equals 2 if $i = 1$, $j = 2$ and $i = 2$, $j = 3$. A slight discrepancy appears for the wall-normal component, $i = j = 2$, for which the model gives

$$\frac{\varepsilon_{22}}{\varepsilon}\frac{k}{\overline{u_2^2}} = 3.5 \tag{2.15}$$

instead of the exact 4. Thus the correction proposed by Launder & Reynolds (1983), which has been used in many low-*Re* second-moment closures to satisfy the exact wall limits of $\varepsilon_{ij}/\overline{u_i u_j}$, is no longer necessary: the wall limits are satisfied directly by considering only the homogeneous portion of the dissipation rate, i.e. using equations (2.13) and (2.14).

The term-by-term scrutiny of expressions (2.13) and (2.14) using the DNS data for $\overline{u_i u_j}$ and ε show that using ε^h leads to a notable improvement: the components of ε_{ij} for the plane channel flow at two Reynolds numbers show excellent agreement with the DNS results, except for a discrepancy in the off-diagonal component ε_{12}, figure 3 (compare with figure 2). Good results, particularly close to the wall, are also obtained for fully developed flow in an axially rotating pipe at various rotation intensities up to $N = W_{wall}/U_m = 10$, figure 4, and for flow behind a backward-facing step. Figure 5 shows results of *a priori* testing at representative locations in all three characteristic regions: in the recirculation bubble, around reattachment and in the recovery zone behind it.

The deficiency in reproducing accurately the off-diagonal components is discussed in more detail in § 5. In channel flows, the only non-zero off-diagonal component ε_{12} is much smaller than the diagonal ones, and this discrepancy is hardly visible in figure 3. However, an enlargement shows a substantial difference in the region of y^+ from 10 to 50, where the DNS data show two peaks, whereas the model gives only one (the same was found for a weakly rotating pipe flow). It is interesting to note that the new model, equations (2.13) and (2.14), reproduces better the off-diagonal components in the non-equilibrium flows considered, with two peaks just as DNS. We return to this problem in § 5, where we propose some remedies that further improve the model for ε_{ij}.

2.4. *Obtaining* ε^h

Equations (2.13) and (2.14) now make it possible to determine ε_{ij}.

To close these expressions it is necessary to provide ε^h. It can be obtained either

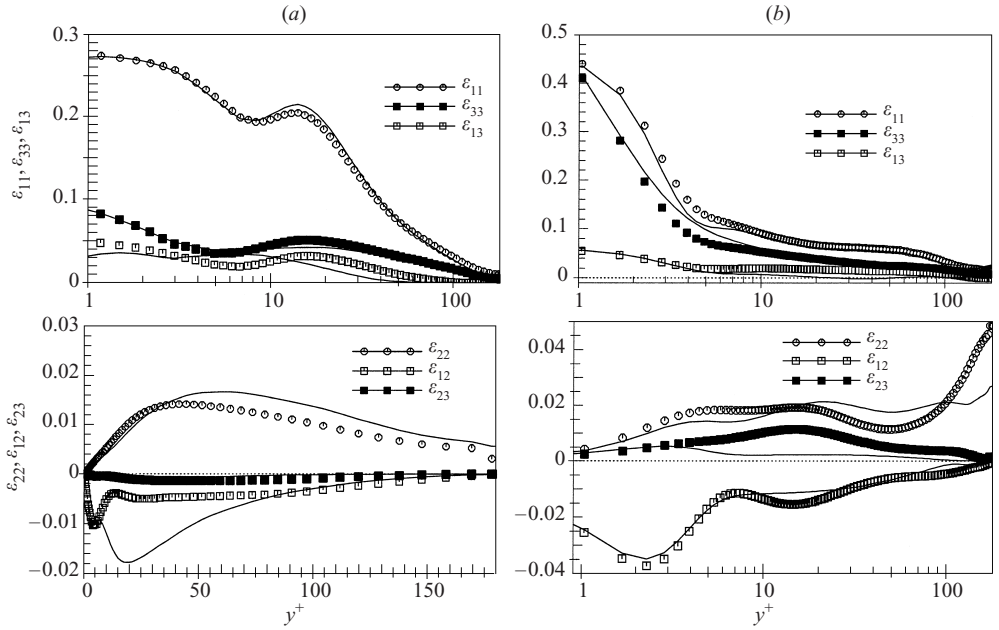

FIGURE 4. Components of ε_{ij} in the fully developed axially rotating pipe flow for different rotation rates. (*a*) $Re_m = 5860$, $N = 0.61$, symbols: DNS Eggels *et al.* (*b*) $Re_m = 4900$, $N = 10$, symbols: DNS Orlandi & Ebstein. Lines: equations (2.13–2.14).

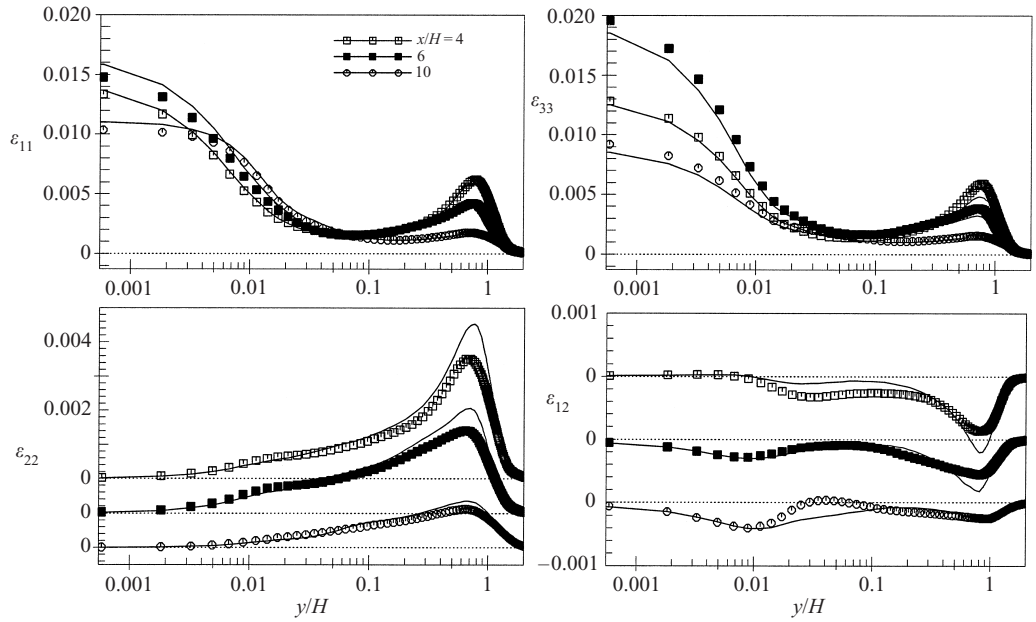

FIGURE 5. Components of ε_{ij} at three locations ($x/H = 4$ – recirculation zone, $x/H = 6$ – reattaching region and $x/H = 10$ – recovery region) in the flow over a backward-facing step. $Re_H = 5100$. Symbols: DNS, Le *et al.* Lines: equations (2.13)–(2.14).

from a conventional low-*Re* ε equation using the fact that

$$\varepsilon^h = \varepsilon - \tfrac{1}{2}\mathscr{D}_k^v, \tag{2.16}$$

or a separate equation for ε^h can be solved. The latter approach is preferred for computational convenience: in fact the stress transport equations can be written with ε_{ij}^h as the sink term with corresponding reduction of the viscous diffusion term by factor of two:

$$\frac{\mathrm{D}\overline{u_i u_j}}{\mathrm{D}t} = \cdots + \frac{1}{2}\underbrace{\frac{\partial}{\partial x_k}\left(\nu\frac{\partial \overline{u_i u_j}}{\partial x_k}\right)}_{\mathscr{D}_{ij}^v} - \varepsilon_{ij}^h + \cdots . \tag{2.17}$$

In such a way we can dispense with the need to compute separately the stress diffusion $\mathscr{D}_{ij}^v$ required for conversion of ε_{ij}^h into ε_{ij} and vice versa (equation (2.13)), thus avoiding possible numerical inaccuracy (computing second derivatives of $\overline{u_i u_j}$)†, except for *a posteriori* validation purposes when comparisons are to be made with data for ε_{ij} or its trace ε. Derivation of the equation for ε^h from the equation for the two-point correlation yields approximately (some higher order terms omitted, Jovanović *et al.* 1995)

$$\frac{\mathrm{D}\varepsilon^h}{\mathrm{D}t} = \frac{\mathrm{D}\varepsilon}{\mathrm{D}t} - \frac{1}{2}\underbrace{\frac{\partial}{\partial x_k}\left(\nu\frac{\partial \varepsilon^h}{\partial x_k}\right)}_{\mathscr{D}_\varepsilon^v}, \tag{2.18}$$

where $\mathrm{D}\varepsilon/\mathrm{D}t$ can be replaced by the right-hand side of the conventional or any other low-*Re* ε equation. It should be noted that the definition of $\tilde{\varepsilon}$ (the 'isotropic' part of the dissipation rate, $\tilde{\varepsilon}|_w = 0$) used in some models to handle the near-wall behaviour and the wall boundary conditions should be modified:

$$\tilde{\varepsilon}^h = \varepsilon^h - \nu\left(\frac{\partial k^{1/2}}{\partial x_n}\right)^2, \quad \varepsilon^h\,|_{x_n=0} = \nu\left(\frac{\partial k^{1/2}}{\partial x_n}\right)^2\Bigg|_{x_n=0}. \tag{2.19}$$

The ε reproduced in a plane channel, using this approach, is very similar to, and in some respects better than, that obtained by the standard formulation. However, in addition to a better physical foundation of the derivation of the ε^h equation, a major advantage is achieved in evaluating the individual dissipation rate components ε_{ij} or ε_{ij}^h, which become important for second-moment closures.

Whatever procedure is adopted, a model for the ε (or ε^h) equation is required. A more accurate term-by-term modelling for this equation is given in the next section. We show that decisive advantages are achieved if the equation for the homogeneous dissipation rate ε^h is solved instead of the total ε, though for some of the terms discussed below this may be irrelevant. In fact, in the final model we abandon completely ε as the scale-providing variable and use instead ε^h, as will be shown below. However, the discussion that follows is applicable equally to ε and ε^h equations.

† The only change in the discretized form of the equations for $\overline{u_i u_j}$ and ε^h is in the contribution to the discretization coefficients by molecular diffusion, which is now devided by factor 2, providing in such a way the (desired) implicit treatment of the non-homogeneous part of the stress dissipation rate.

3. Term-by-term modelling of the ε (and ε^h) equation

The exact equation for the dissipation rate can be written as

$$\frac{\mathrm{D}\varepsilon}{\mathrm{D}t} = \underbrace{-2\nu\left(\overline{\frac{\partial u_i}{\partial x_l}\frac{\partial u_k}{\partial x_l}} + \overline{\frac{\partial u_l}{\partial x_i}\frac{\partial u_l}{\partial x_k}}\right)\frac{\partial U_i}{\partial x_k}}_{P_\varepsilon^1 + P_\varepsilon^2} \underbrace{-2\nu\overline{u_k\frac{\partial u_i}{\partial x_l}}\frac{\partial^2 U_i}{\partial x_k \partial x_l}}_{P_\varepsilon^3}$$

$$\underbrace{-2\nu\overline{\frac{\partial u_i}{\partial x_k}\frac{\partial u_i}{\partial x_l}\frac{\partial u_k}{\partial x_l}}}_{P_\varepsilon^4} \underbrace{-2\overline{\left(\nu\frac{\partial^2 u_i}{\partial x_k \partial x_l}\right)^2}}_{Y}$$

$$\underbrace{+\frac{\partial}{\partial x_k}\left(\nu\frac{\partial \varepsilon}{\partial x_k}\right)}_{\mathscr{D}_\varepsilon^\nu} \underbrace{+\frac{\partial}{\partial x_k}\left(-\overline{u_k\varepsilon'}\right)}_{\mathscr{D}_\varepsilon^t} \underbrace{+\frac{\partial}{\partial x_k}\left(-\frac{2\nu}{\rho}\overline{\frac{\partial p}{\partial x_i}\frac{\partial u_k}{\partial x_i}}\right)}_{\mathscr{D}_\varepsilon^p}, \qquad (3.1)$$

$$\underbrace{\qquad\qquad\qquad\qquad\qquad\qquad\qquad\qquad\qquad\qquad}_{\mathscr{D}_\varepsilon}$$

with conventional notation for different terms. The physical meaning of the terms can be found, e.g. in the paper by Mansour *et al.* (1988).

A reformulation of some of the terms in the ε equation is now described.

3.1. *The mixed production term*

First consider the 'mixed' production term

$$P_\varepsilon^1 + P_\varepsilon^2 = -2\nu\left(\overline{\frac{\partial u_i}{\partial x_l}\frac{\partial u_j}{\partial x_l}} + \overline{\frac{\partial u_l}{\partial x_i}\frac{\partial u_l}{\partial x_j}}\right)\frac{\partial U_i}{\partial x_j}. \qquad (3.2)$$

This term is regarded as negligible in high-Re flows. The major production of ε, $P_{\varepsilon 4}$, associated with the self-stretching of the fluctuating vortices is usually modelled in terms of the energy production $P_k = -\overline{u_i u_j}\partial U_i/\partial x_j$, scaled with the characteristic turbulence time scale k/ε.

It should be recalled that the first term in the bracket is in fact ε_{ij}. The second term is closely related to ε_{ij} – they contain common terms. DNS data for near-wall flows show that ε_{ij} remains anisotropic beyond the viscosity-affected wall region, even at higher Re. Now, if ε_{ij} can be modelled satisfactorily by equation (2.13), this term can be retained in its exact form. Of course, away from the wall and at high Re, ε_{ij} becomes isotropic irrespective of the stress anisotropy and this term is not sufficient to account for total production of ε so that the standard production term should be retained, although with a smaller coefficient. Figure 6 presents a new production model in a plane channel. The new model consists of the sum of the new and the standard terms, the latter with $C_{\varepsilon 1} = 1$:

$$P_\varepsilon^1 + P_\varepsilon^2 = -\varepsilon_{ij}\frac{\partial U_i}{\partial x_j} - 1.0\,\overline{u_i u_j}\frac{\partial U_i}{\partial x_j}\frac{\varepsilon}{k}. \qquad (3.3)$$

Note that the same value, $C_{\varepsilon 1} = 1$, was advocated recently both by Craft & Launder (1996) and Speziale & Gatski (1997), though each in the context of their ε-equations, which differ from each other and from the one considered here.

In addition to better reproduction of the exact terms than achieved by the standard term alone with $C_{\varepsilon 1} = 1.44$, the new model offers additional flexibility, which should

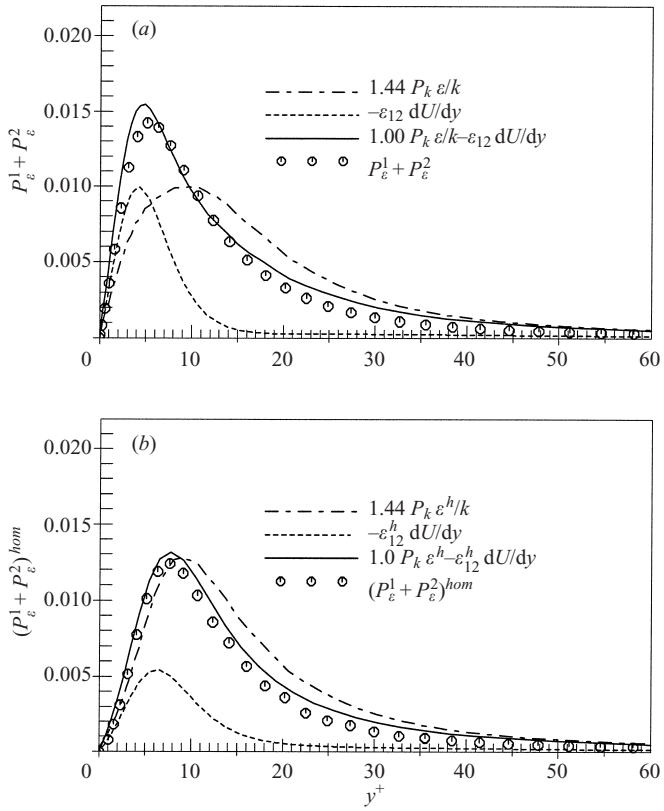

FIGURE 6. New model of mixed production $P^1_\varepsilon + P^2_\varepsilon$: (*a*) for the conventional ε equation, and (*b*) for the new ε^h equation. Plane channel flow, $Re_m = 5600$. Symbols: DNS data, Kim *et al.*

be particularly useful in non-equilibrium flows subjected to strong linear straining. This becomes obvious if P^1_ε is expanded into components. For two-dimensional flows

$$P^1_\varepsilon = -\varepsilon_{12}\frac{\partial U_1}{\partial x_2} - (\varepsilon_{11} - \varepsilon_{22})\frac{\partial U_1}{\partial x_1}. \tag{3.4}$$

Recall that the conventional model of the production of ε, $P_\varepsilon = C_{\varepsilon 1}P_k\varepsilon/k$, fails in reproducing non-equilibrium flows, particularly with strong irrotational strain (e.g. axisymmetric contraction, boundary layers in strong pressure gradients). Hanjalić & Launder (1980) proposed sensitizing the production P_ε to irrotational strain by increasing the coefficient $C_{\varepsilon 1}$ from 1.44 to $C'_{\varepsilon 1} \approx 4.44$,† and introduced a new term, $(C'_{\varepsilon 1} - C_{\varepsilon 1})C_\mu k\Omega_{ij}\Omega_{ij}$ (where Ω_{ij} is mean flow rotation tensor), which ensured that the model reduces to the conventional form in equilibrium thin shear flows, where $\overline{u_1u_2} \approx -C_\mu^{1/2}k$, with $C_\mu = 0.09$. The net effect is visible in two-dimensional flows, where in addition to the conventional production, another source term, $(C'_{\varepsilon 1} - C_{\varepsilon 1})(\overline{u_1^2} - \overline{u_2^2})k/\varepsilon\partial U_1/\partial x_1$, appears in the ε-equation.

We show here that such an enhancement of the production of ε is now accounted for by the new formulation of P^1_ε, and no additional term is necessary. While $\overline{u_1u_2}/(\overline{u_1^2} - \overline{u_2^2})$ is of the order of magnitude of 1, making the production by both the rotational and irrotational strain of equal importance, $\varepsilon_{12}/(\varepsilon_{11} - \varepsilon_{22})$ is much smaller than 1, except

† Later, some authors adopted different values e.g. Jakirlić & Hanjalić (1995) used $C'_{\varepsilon 1} = 2.6$.

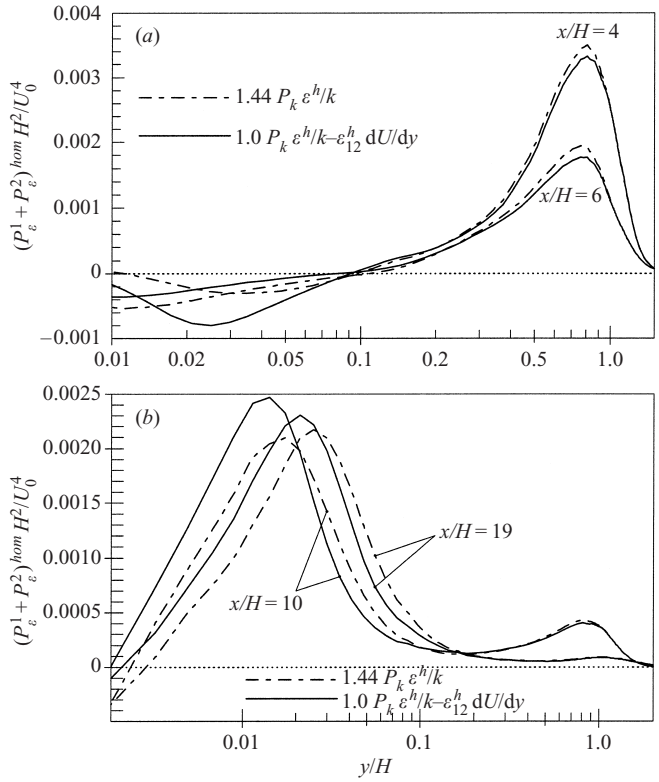

FIGURE 7. Comparison of the new and traditional models of mixed production $P^1_\varepsilon + P^2_\varepsilon$ for the new ε-equation at several locations in the flow over a backward-facing step. $Re_H = 5000$, from DNS Le *et al.*

very close to the wall (Hanjalić & Jakirlić 1993). Hence, the term will itself distinguish the effect of the irrotational from the rotational strain in the production of ε.

Unfortunately, no information about individual terms in the exact equation for ε is available for any other flows. Hence, further direct validation of the model proposed above for $P^1_\varepsilon + P^2_\varepsilon$ in more complex flows remains to be done. However, some insight can be gained by comparing the terms in the model equation (3.3) with the conventional model of the production of ε, i.e.

$$P^1_\varepsilon + P^2_\varepsilon = 1.44 P_k \frac{\varepsilon}{k}. \tag{3.5}$$

Figures 6 to 8 show such a comparison for fully developed plane channel flows, several positions in a backward-step flow, and for fully developed axially rotating pipe. The conventional model drastically underestimates the total DNS production in a channel flow, which is compensated by the model of the sink term Y, which is also underestimated as shown in figure 11(a) (see also figures 23 and 24 in Mansour *et al.* 1988). Hence, the present disagreement between the new and conventional model is expected. In contrast, the new model of $P^1_\varepsilon + P^2_\varepsilon$, equation (3.3) reproduces very well the DNS data for a plane channel, both using the total dissipation ε, figure 6(a), or homogeneous dissipation ε^h, figure 6(b). The DNS results in figure 6(b) and for other terms in the ε^h equation discussed in the the following sections are from Jovanović *et al.* (1995), which were derived from the DNS results of Kim, Moin & Moser (1987). It

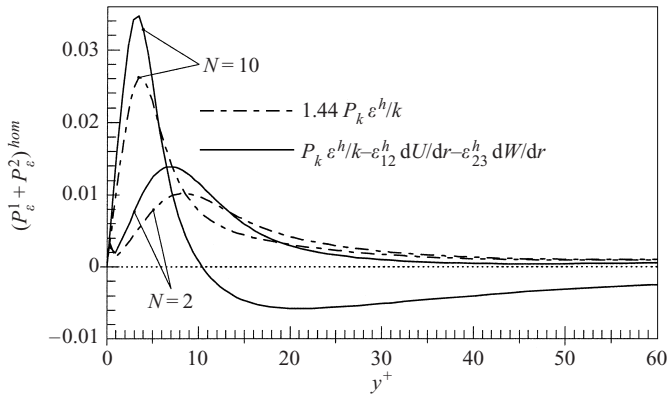

FIGURE 8. Comparison of the new and traditional models of mixed production $P_\varepsilon^1+P_\varepsilon^2$ for the new ε-equation for several rotation rates in fully developed axially rotating pipe flow, $Re_m = 4900$, DNS: Orlandi & Ebstein.

is worth noting that the term P_ε^1 becomes smaller if ε^h is used, reducing the difference between the new model, equation (3.3), and the conventional model, equation (3.5) (solid and chain lines in figure 6). Figures 7 and 8 show only the comparison between the new and conventional models, equations (3.3) and (3.5), for several positions within the separation bubble and recovery region in a backward-step flow, and in a rotating pipe for two rotation numbers, using ε^h. Note the new term with tangential velocity derivative in figure 8, which produces a substantial difference in rotating pipe flow. No DNS data are available for the budget of ε, so that a direct validation is not possible.

3.2. *The gradient production term*

Term P_ε^3, referred as the gradient production of ε, is defined as

$$P_\varepsilon^3 = -2\nu\overline{u_k\frac{\partial u_i}{\partial x_l}}\frac{\partial^2 U_i}{\partial x_k\partial x_l}. \tag{3.6}$$

Current practice assumes a simple gradient model $\overline{u_k\partial u_i/\partial x_l} \propto \tau\overline{u_ju_k}(\partial^2U_i/\partial x_j\partial x_l)$, where $\tau = k/\varepsilon$, yielding the term with the squared second velocity derivative. The expression follows from the Taylor vorticity transport approach and is a rigid constraint because it does not allow for a proper sign of the curvature of the mean velocity profile. Bernard's vorticity transport theory (Bernard 1990) provides a more rational method (J. R. Ristorcelli, private communication). The turbulent velocity gradient flux is expanded into

$$\overline{u_k\frac{\partial u_i}{\partial x_l}} = \left(\frac{\partial\overline{u_ku_i}}{\partial x_l} - \overline{u_i\frac{\partial u_k}{\partial x_l}}\right) = \left(\frac{\partial\overline{u_ku_i}}{\partial x_l} - \overline{u_is_{kl}} - \overline{u_i\omega_{kl}}\right), \tag{3.7}$$

where s_{kl} and ω_{kl} are the fluctuating strain rate and vorticity respectively. The first term is now exact. The second term needs modelling. The third term is omitted since it is antisymmetric in its indices while the velocity curvature term is symmetric. For the two-dimensional near-equilibrium wall layer

$$\frac{\partial^2U_i}{\partial x_k\partial x_l} = \frac{\partial^2U_1}{\partial x_2\partial x_2}\delta_{i1}\delta_{k2}\delta_{l2}, \tag{3.8}$$

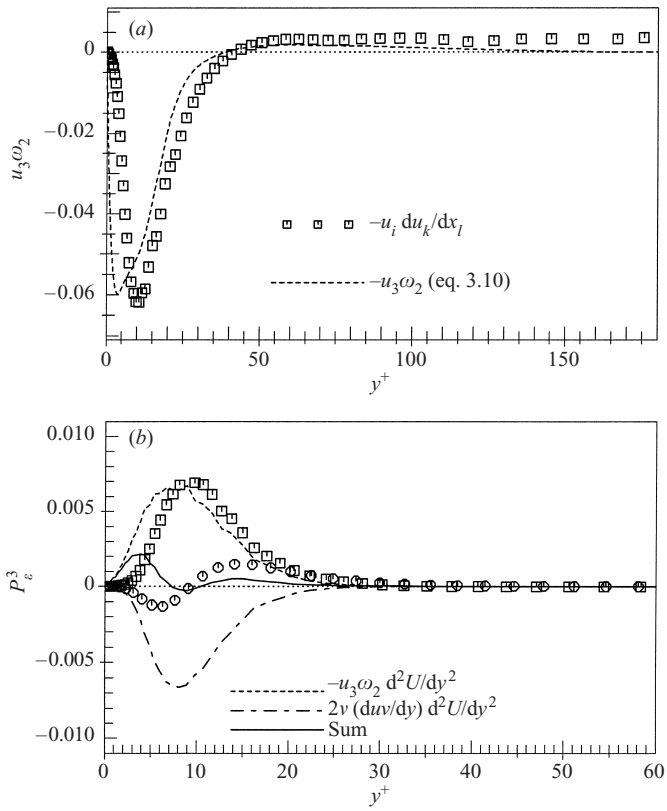

FIGURE 9. The new model of (*a*) vorticity flux $\overline{u_3\omega_2}$ (equation (3.10), $Q_3 = 0.65$, $Q_4 = 10.8$) and (*b*) the 'gradient' production P^3_ε. Plane channel flow, $Re_m = 5600$. Symbols: DNS from Kim *et al.*

the term $\overline{u_1 s_{22}}$ can be expanded, using the continuity equation, to produce

$$\overline{u_1 s_{22}} = -\frac{1}{2}\frac{\partial(\overline{u_1^2} - \overline{u_3^2})}{\partial x_1} - \frac{\partial \overline{u_1 u_3}}{\partial x_3} - \overline{u_3\omega_2}, \tag{3.9}$$

where $\omega_i = -\epsilon_{ijk}(\partial u_j/\partial x_k)$. The first two terms can be neglected because of spanwise and streamwise homogeneity. The results of Bernard (1990) are used to close $\overline{u_3\omega_2}$:

$$\overline{u_3\omega_2} = \frac{1}{2}\frac{Q_4}{1 + Q_3 Q_4(\partial U_1/\partial x_2)^2}\frac{\partial \overline{u_3^2}}{\partial x_2}\frac{\partial U_1}{\partial x_2}, \tag{3.10}$$

where Q_3 and Q_4 are the Lagrangian integral scales, defined as $\int_\tau^0 S_{ijk}(t)/S_{ijk}(0)\mathrm{d}t$ for non-zero components of the time correlation $S_{ijk} = \overline{u_i(t_0)\partial u_j(t_0 + t)/\partial x_k}$. For a fully developed channel flow, Bernard (1990) recommended $Q_3 = 0.65$ and $Q_4 = 10.8$.

The profile of $\overline{u_3\omega_2}$ obtained from expression (3.10) for the channel flow is compared with the DNS data in figure 9(*a*). The agreement seems qualitatively acceptable. However, the insertion of $\overline{u_3\omega_2}$ in equation (3.7) and subsequently in equation (3.6) for the complete production term yields P^3_ε which differs both in magnitude and in sign from the DNS results in the near-wall region, figure 9(*b*).

A substantial improvement is achieved if $\partial\overline{u_3^2}/\partial x_2$ is replaced by $\partial\overline{u_2^2}/\partial x_2$, and the Bernard time-scale function $Q_4/(1 + Q_3 Q_4(\partial U_1/\partial x_2)^2)$ by k/ε, figure 10(*a*), yielding

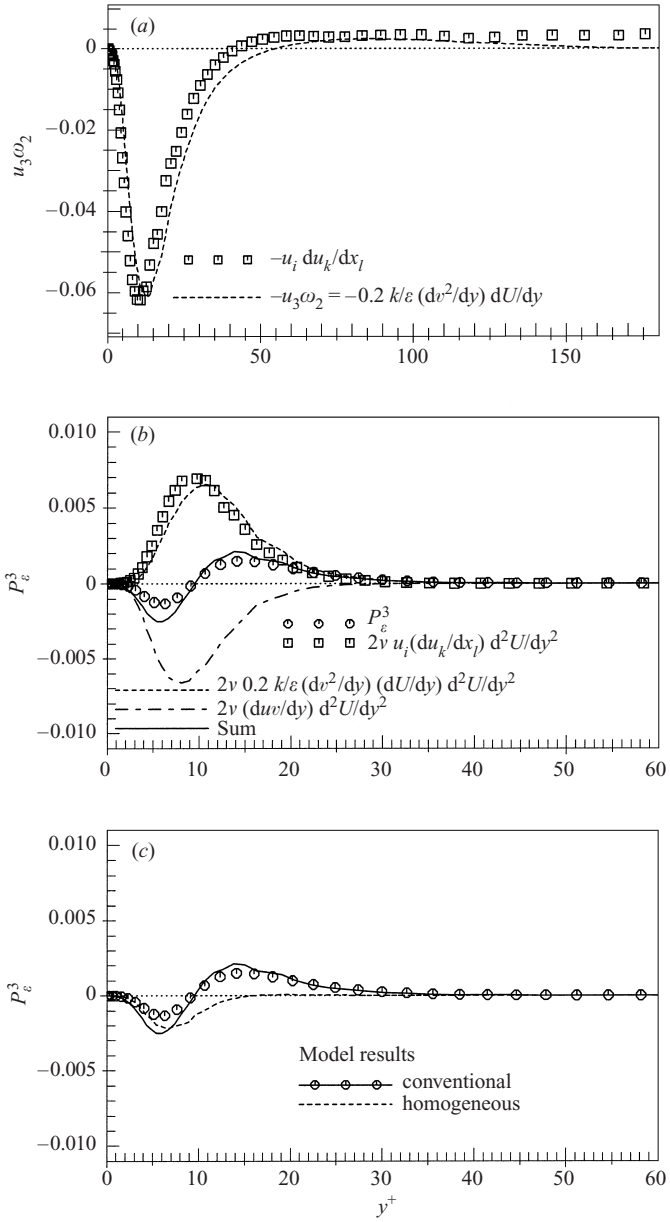

FIGURE 10. The modified new model of (*a*) vorticity flux $\overline{u_3\omega_2}$, (*b*) the 'gradient' production P^3_ε for the conventional ε equation and (*c*) its comparison with the homogeneous version. Plane channel, $Re = 5600$. Symbols: DNS from Kim *et al.*

the expression for P^3_ε

$$P^3_\varepsilon = -2\nu\frac{\partial\overline{u_1u_2}}{\partial x_2}\frac{\partial^2U_1}{\partial x_2\partial x_2} - 0.4\nu\frac{k}{\varepsilon}\frac{\partial\overline{u_2^2}}{\partial x_2}\frac{\partial U_1}{\partial x_2}\frac{\partial^2U_1}{\partial x_2\partial x_2}. \tag{3.11}$$

The plot of each term in expression (3.11) and of their sum, i.e. the complete model of P^3_ε computed from DNS data for a plane channel, is presented in figure 10(*b*),

showing good agreement with the DNS. Figure 10(*c*) shows the comparison of this term with its homogeneous counterpart $P_{\varepsilon^h}^3$ (dashed line).

Note that the expression (3.10) reduces to that proposed by Rodi & Mansour (1993), which was derived in the framework of the $k-\varepsilon$ model, if $\partial\overline{u_3^2}/\partial x_2$ is replaced by $\partial k/\partial x_2$. For a general second-moment closure, (3.11) can be generalized into the tensor invariant form

$$P_\varepsilon^3 = -2\nu\left(\frac{\partial\overline{u_k u_i}}{\partial x_l}\frac{\partial^2 U_i}{\partial x_k \partial x_l} + C_{\varepsilon 3}\frac{k}{\varepsilon}\frac{\partial\overline{u_k u_l}}{\partial x_j}\frac{\partial U_i}{\partial x_k}\frac{\partial^2 U_i}{\partial x_j \partial x_l}\right), \tag{3.12}$$

where $C_{\varepsilon 3} = 0.2$.

3.3. *Production–destruction term*

For the two remaining terms, representing the difference between the turbulent production and viscous destruction of ε, which represents the major source of dissipation at high *Re*, Hanjalić & Launder (1976) proposed a joint model

$$P_\varepsilon^4 - Y = -2\nu\overline{\frac{\partial u_i}{\partial x_k}\frac{\partial u_i}{\partial x_l}\frac{\partial u_k}{\partial x_l}} - 2\overline{\left(\nu\frac{\partial^2 u_i}{\partial x_k \partial x_k}\right)^2} = -C_{\varepsilon 2} f_\varepsilon \frac{\varepsilon\tilde{\varepsilon}}{k}, \tag{3.13}$$

where $\tilde{\varepsilon} = \varepsilon - 2\nu(\partial k^{1/2}/\partial x_l)^2$. The plot of expression (3.13) with the original function f_ε and the modified one proposed by Coleman & Mansour (1993), shows poor agreement close to the wall for both models, figure 11(*a*). For illustration, the proposal of Durbin to replace in the model (3.13) the time scale $\tau = k/\varepsilon$ by the Kolmogorov scale $\tau_K = \sqrt{\nu/\varepsilon}$, when τ_K becomes larger than $\tau/6$, is presented, also showing poor agreement. In contrast, the application of the same model using the homogeneous dissipation rate, i.e. $-C_{\varepsilon 2} f_\varepsilon \varepsilon^h \tilde{\varepsilon}^h/k$, where $\tilde{\varepsilon}^h = \varepsilon^h - \nu(\partial k^{1/2}/\partial x_l)^2$ (2.19), yields much better agreement with the DNS data, as shown in figure 11(*b*).

3.4. *Balance of the production and destruction terms*

What we need is the sum of all source and sink terms in the equation, which balances the convection and diffusion. Figure 12 shows the sum $P_\varepsilon^1 + P_\varepsilon^2 + P_\varepsilon^3 + P_\varepsilon^4 - Y$ for fully developed plane channel flow. As expected, because of zero convection and small diffusion (see below), this sum is small all across the flow. In spite of the very good *a priori* reproduction of the individual terms shown above, the plot of their sum on an expanded scale displays some small imperfections, and agreement with the DNS data is not perfect, especially in the buffer region for y^+ between 7 and 18 for the *Re* considered. However, with the new ε^h equation, agreement is substantially improved and is much closer than with the conventional ε equation. In more complex, non-equilibrium flows, where the transport terms are significant and where the imposed flow conditions (strain rate, pressure gradient, body forces) will cause different source terms to depart from equilibrium, the importance of reproducing accurately the individual terms should matter and hopefully the total sum of source terms should agree better. Unfortunately, due to the lack of DNS (or other) data for individual

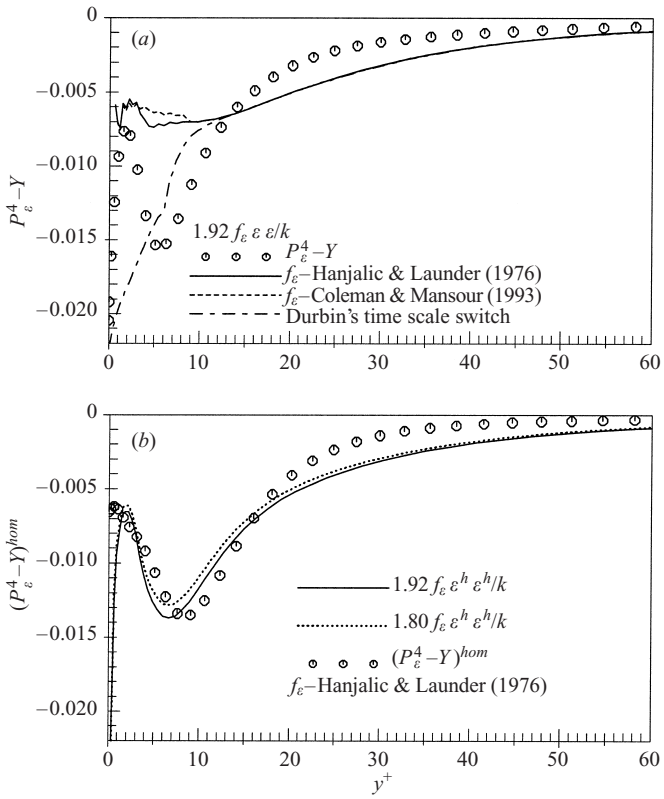

FIGURE 11. Model of $P^4_\varepsilon - Y$ for (a) the conventional and (b) the new ε equation. Plane channel, $Re_m = 5600$. Symbols: DNS data from Kim *et al.*

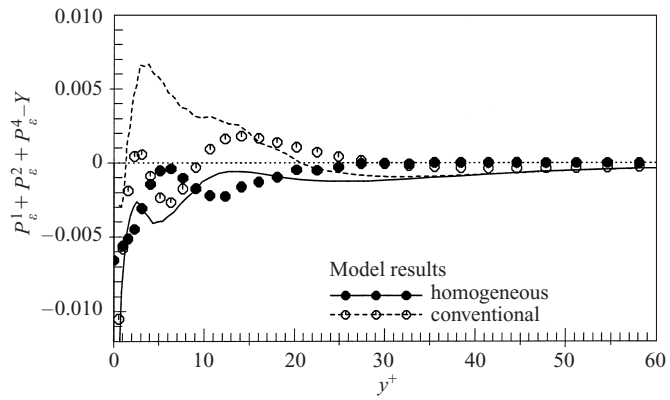

FIGURE 12. Balance between production and destruction terms, $P^1_\varepsilon + P^2_\varepsilon$, P^3_ε and $P^4_\varepsilon - Y$, in the ε and ε^h equations. Plane channel, $Re_m = 5600$. Symbols: DNS from Kim *et al.*

terms in ε or ε^h equation in flows other than in a plane channel makes it at present impossible to validate this expectation. The only way to test the model is to verify the outcome of model application by comparing the mean-flow parameters and the second moments computed from the complete model with the available DNS and experimental results. This is presented in § 4.

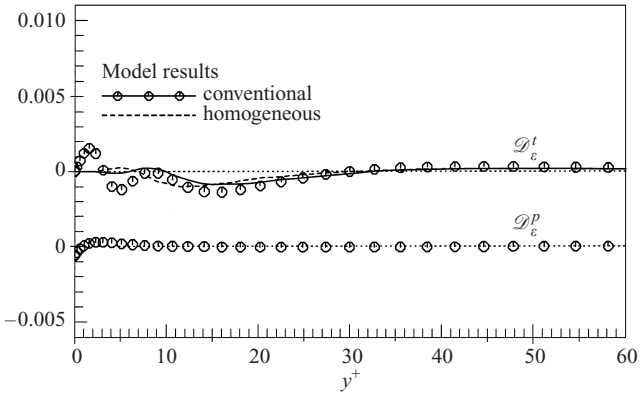

FIGURE 13. Turbulent ($\mathscr{D}_\varepsilon^t$) and pressure ($\mathscr{D}_\varepsilon^p$) transport terms in the ε equation. Plane channel, $Re_m = 5600$. Symbols: DNS data from Kim *et al.*

3.5. *Transport terms*

The term $\mathscr{D}_\varepsilon^t$, representing diffusion transport of ε due to velocity fluctuations, is commonly modelled by applying the general gradient diffusion hypothesis (Daly & Harlow 1970):

$$\mathscr{D}_\varepsilon^t = \frac{\partial}{\partial x_k}\left[C_\varepsilon \frac{\varepsilon}{k}\overline{u_k u_l}\frac{\partial \varepsilon}{\partial x_l}\right]. \tag{3.14}$$

The plot of this term compared with the DNS results, figure 13, shows a poor agreement in the immediate wall vicinity: $y^+ < 10$. Bearing in mind that the contribution of this term to the overall budget of the ε equation is weak when compared with the production and destruction terms (see previous sections), this simple formulation was also applied to model homogeneous dissipation (dashed line in figure 13). For completeness, the pressure transport term $\mathscr{D}_\varepsilon^p$ obtained by DNS (Mansour *et al.* 1988) is also displayed in figure 13. Because of its small value, this term was not further considered.

3.6. *The complete ε^h equation*

The final form of the new model dissipation equation, expressed solely in terms of ε^h can now be written as

$$\frac{\mathrm{D}\varepsilon^h}{\mathrm{D}t} = \underbrace{-\varepsilon_{ij}^h \frac{\partial U_i}{\partial x_j} - \overline{u_i u_j}\frac{\partial U_i}{\partial x_j}\frac{\varepsilon^h}{k}}_{P_{\varepsilon^h}^1 + P_{\varepsilon^h}^2} \underbrace{-2\nu\left(\frac{\partial \overline{u_i u_k}}{\partial x_l}\frac{\partial^2 U_i}{\partial x_k \partial x_l} + C_{\varepsilon 3}\frac{k}{\varepsilon^h}\frac{\partial \overline{u_k u_l}}{\partial x_j}\frac{\partial U_i}{\partial x_k}\frac{\partial^2 U_i}{\partial x_j \partial x_l}\right)}_{P_{\varepsilon^h}^3}$$

$$\underbrace{-C_{\varepsilon 2} f_\varepsilon \frac{\varepsilon^h \tilde{\varepsilon}^h}{k}}_{P_{\varepsilon^h}^4 - Y} + \underbrace{\frac{\partial}{\partial x_k}\left[\left(\frac{1}{2}\nu\delta_{kl} + C_\varepsilon \frac{\varepsilon^h}{k}\overline{u_k u_l}\right)\frac{\partial \varepsilon^h}{\partial x_l}\right]}_{\frac{1}{2}\mathscr{D}_{\varepsilon^h}^v + \mathscr{D}_{\varepsilon^h}^t}. \tag{3.15}$$

It is noted that in spite of its extended form with several additional terms compared with the conventional equation for high-Reynolds-number flows, equation (3.15) contains only three empirical coefficients.

This equation can now be solved with the model equation for turbulent stress $\overline{u_i u_j}$ that contains conventional modifications for near-wall and viscosity effects, but with

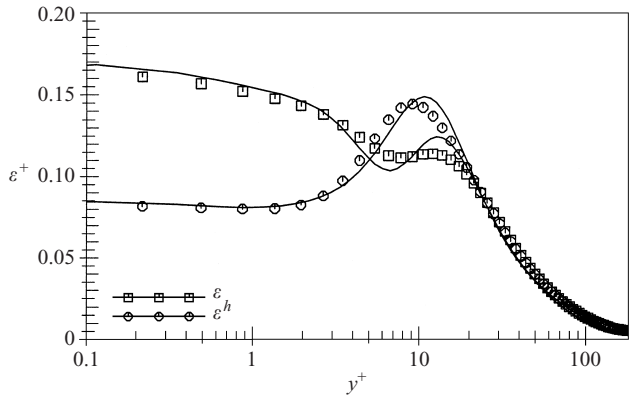

FIGURE 14. Computed ε^h and ε in fully developed channel flow by the new model of the ε^h equation (only the ε^h equation was solved). Plane channel, $Re_m = 5600$. Symbols: DNS data from Kim *et al.*

ε_{ij}^h as the sink term and with the factor $1/2$ in front of the viscous diffusion term, as follows from equation (2.13). Note that the full dissipation rate ε does not appear at all in the model and need not be considered.

In the following section we present some results for several flows computed with the new ε^h equation in conjunction with the low-Reynolds-number equations for $\overline{u_i u_j}$ of Jakirlić & Hanjalić (1995) and Hanjalić & Jakirlić (1998). The full set of equations and coefficients is given in Appendix A.

4. Illustration of model performance

Despite faithful *a priori* reproduction of the dissipation tensor components ε_{ij}, i.e. ε_{ij}^h (equations (2.6) and (2.14)), and of each term in the ε^h equation (3.15), these models can gain full credibility only if solved numerically in the framework of a full computational scheme, i.e. in conjunction with a model Reynolds-stress equation.

First, only the transport equation for the 'homogeneous' energy dissipation rate ε^h was numerically integrated, using the DNS data for all input variables. The final outcome is shown in figures 14 and 15 where the reproduction of ε^h and of the total ε by solving the new equation is presented for a plane channel flow and a flow in an axially rotating pipe.

Whereas the results obtained for a plane channel flow agree very well with the DNS data, this is not the case for the axially rotating pipe flow. This is especially visible in the immediate wall vicinity ($y^+ \leqslant 5$). The most likely reason lies in the DNS data for Reynolds stresses, which were used as input variables. They are obviously not absolutely exact, bearing in mind that wall values of both energy dissipation rates, ε and ε^h, are completely determined by the streamwise and lateral normal stress components, $\overline{u_1 u_1}$ and $\overline{u_3 u_3}$ respectively (see further discussion). The effect of the Rubinstein & Zhou (1997) term, causing reduction of the dissipation rate level in rotational flows, is also illustrated in these figures.

Further illustrations, using the full model in conjunction with the HJ low-Reynolds-number transport equation for $\overline{u_i u_j}$ (see the Appendix), are provided in figures 16 to 19 for fully developed channel and pipe flows, zero-pressure-gradient boundary layers, flow in an axially rotating pipe, and for flow over a backward-facing step.

We regard these results in general as satisfactory, particularly in view of the fact that a single model with a single set of empirical coefficients and functions

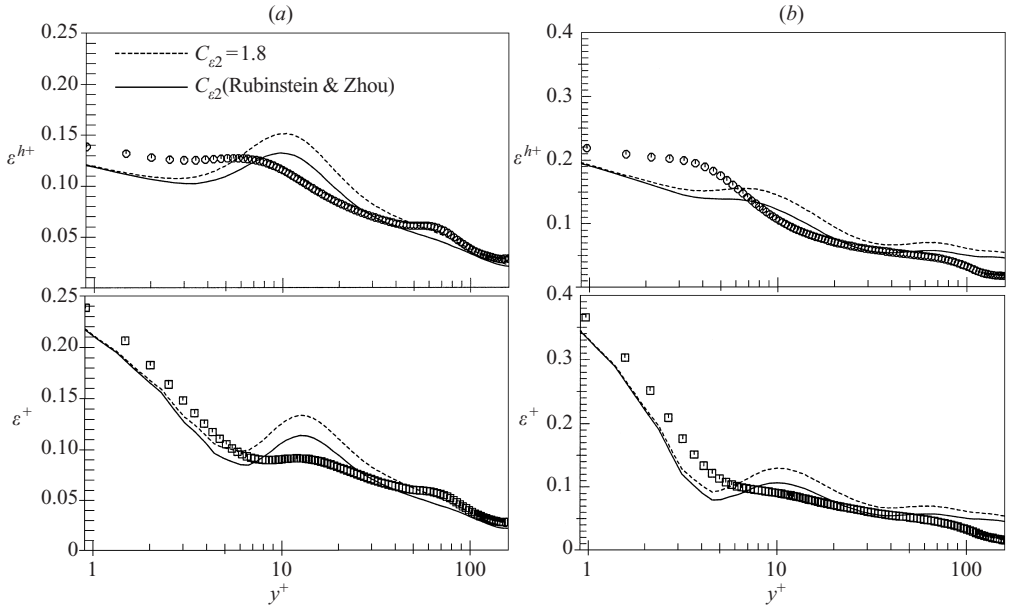

FIGURE 15. Computed ε^h and ε in fully developed flow in an axially rotating pipe for different rotation rates by the new model of the ε^h equation (only the ε^h equation was solved). $Re_m = 4900$. Symbols: DNS data of Orlandi & Ebstein. (*a*) $N = 2$, (*b*) $N = 5$.

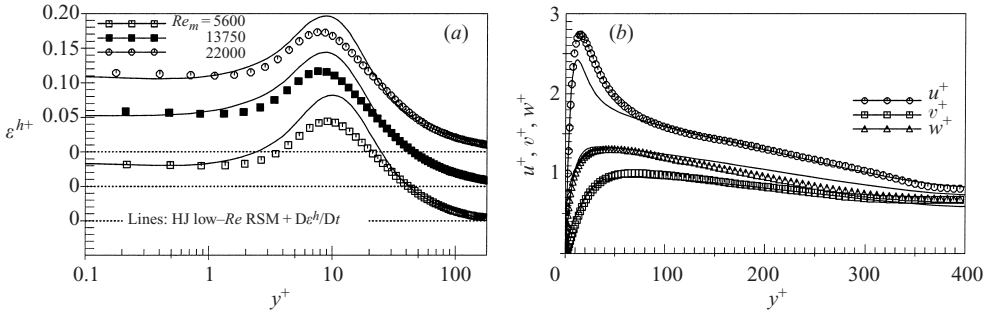

FIGURE 16. Computed (*a*) ε^h and (*b*) normal stress components for $Re_m = 13\,750$ in fully developed channel flow using the new model of the ε^h equation in the framework of HJ low-*Re* Reynolds stress model (RSM). Symbols: DNS of Kim *et al.*

was used to compute several flows with distinct mean flow and turbulence features, including separation, reattachment and flow rotation. Generally, there is still room for improvement, e.g. for rotating pipe (figure 18) and for better reproducing the DNS value of dissipation at the wall (figures 17 and 18). The latter, however, cannot be attributed to the ε^h equation, but to the model of the pressure–strain and pressure diffusion, which balance the (exact) viscous diffusion and dissipation rate in the near-wall region. The predicted behaviour of turbulent stresses governs the boundary conditions for ε^h, and thus influences its predicted near-wall behaviour: $\varepsilon^h_{wall} = \frac{1}{2}(\overline{b_1 b_1} + \overline{b_3 b_3})$, where $\overline{b_1 b_1}$ and $\overline{b_3 b_3}$ are coefficients in the Taylor-series expansion of $\overline{u_1 u_1}$ ($\overline{u_1 u_1} = \overline{b_1 b_1} y^{+2} + \cdots$) and $\overline{u_3 u_3}$ ($\overline{u_3 u_3} = \overline{b_3 b_3} y^{+2} + \cdots$) respectively. For example, the model slightly underpredicts $\overline{u_3 u_3}$, as seen in figure 18 (denoted as w), which in turn yields smaller values of ε^h at the wall. Hence, the results presented should serve

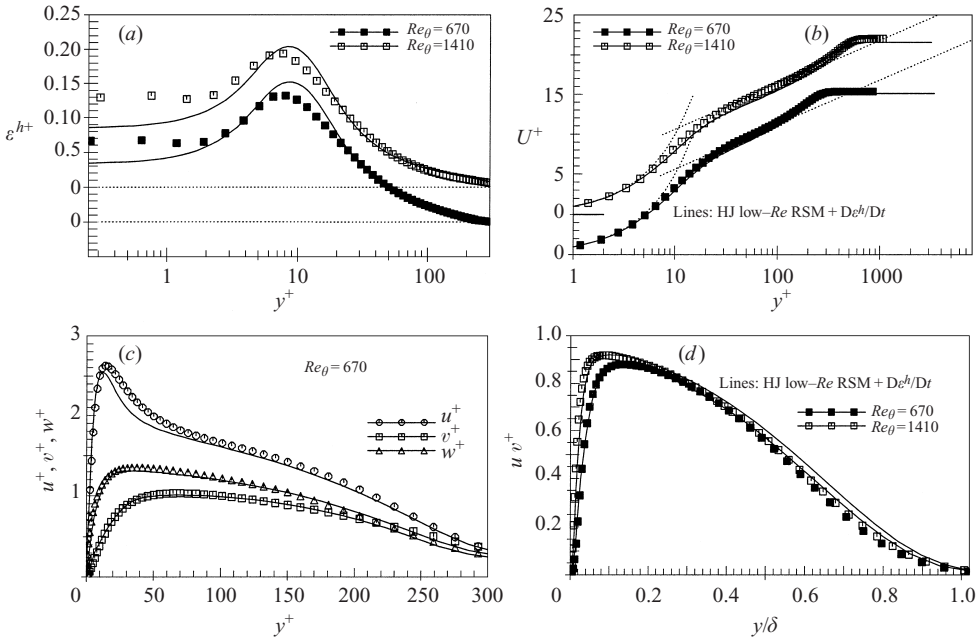

FIGURE 17. Computed (*a*) ε^h, (*b*) mean velocity and (*c*, *d*) stress components in the zero pressure gradient boundary layer using the new model of the ε^h equation in the framework of HJ low-*Re* RSM. Symbols: DNS from Spalart.

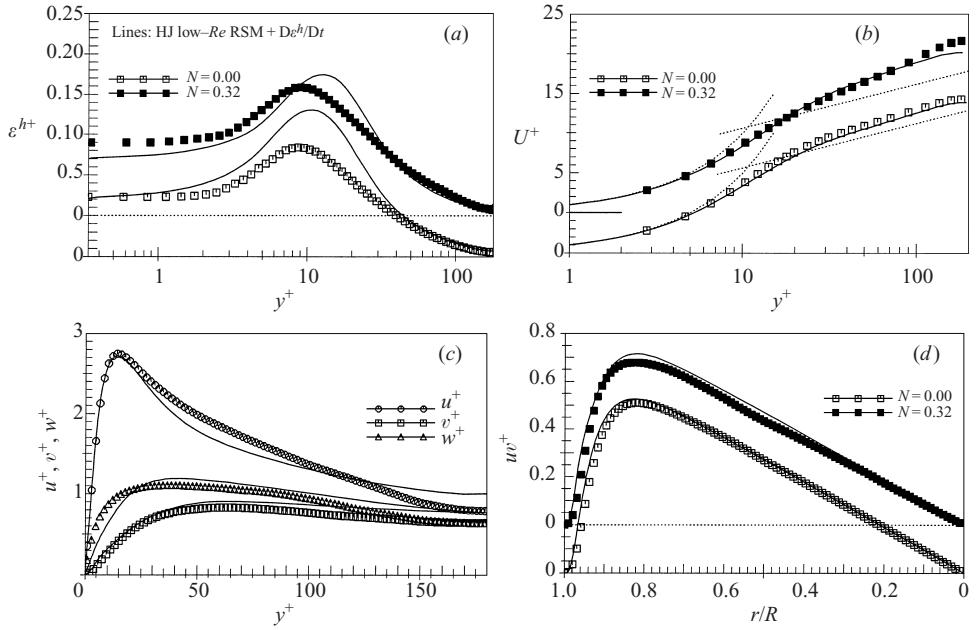

FIGURE 18. Computed (*a*) ε^h, (*b*) mean velocities and (*c*, *d*) stress components in an axially rotating pipe flow ($N = 0$ and $N = 0.32$) using the new model of the ε^h equation in the framework of HJ low-*Re* RSM. Symbols: DNS Eggels *et al.*

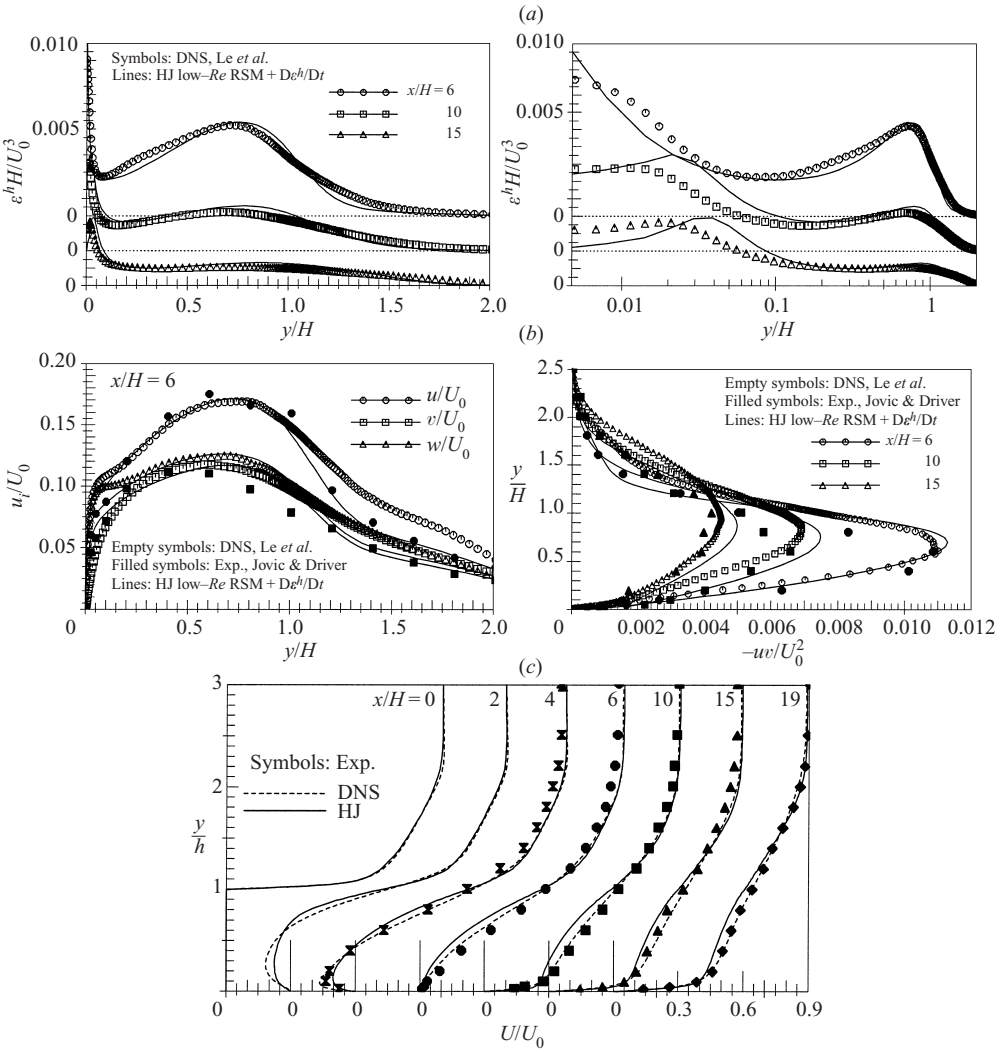

FIGURE 19. Computed (*a*) ε^h, (*b*) stress components and (*c*) mean velocities at selected locations in the flow over a backward-facing step using the new model of the ε^h equation in the framework of HJ low-*Re* RSM. $Re_H = 5000$, $ER = 1.2$.

as an illustration of the potential of the new model for ε^h and ε^h_{ij} which, in principle, can be used in conjunction with other low-Reynolds-number second-moment or eddy-viscosity closures.

These results are admittedly slightly inferior for the near-wall region compared with results shown in figures 3 to 5, obtained in an *a priori* way. Two sources of discrepancy were discovered: the inadequacy of the model of the off-diagonal components of ε^h_{ij}, and a slight imbalance of the model equation for the wall-normal stress component $\overline{u_2 u_2}$ at the wall (related to equation (2.15)). Although the off-diagonal components of ε^h_{ij} are small compared with the diagonal ones in wall-equilibrium and backward-step flows – though not in a rotating pipe, their proper modelling becomes important if the new model of the mixed production, equation (3.3), is to be used. We discuss some possible improvements of the model for ε^h_{ij} that will remedy this deficiency in the next section. Fortunately, the use of ε^h as the scale-providing variable reduces the

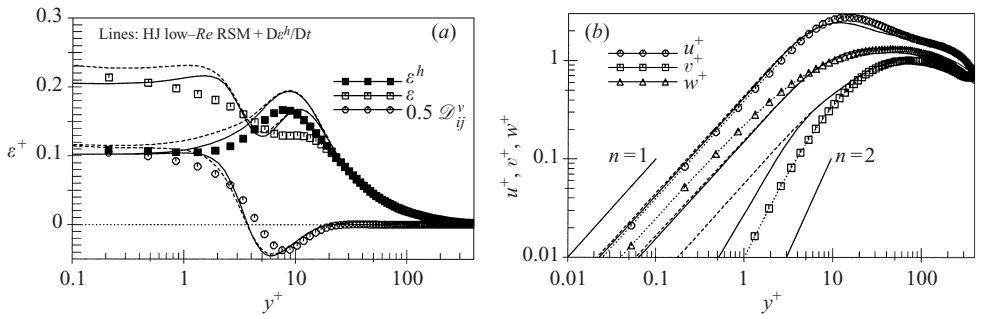

FIGURE 20. Computed (*a*) ε^h, ε and $0.5\dot{\mathscr{D}}^v_{ij}$ and (*b*) blow up of normal Reynolds stress components in the fully developed channel flow using the new model of the ε^h-equation in the framework of HJ low-*Re* RSM. $Re_m = 13\,750$. Symbols: DNS, Kim *et al.* Solid lines: with D^p_{ij}, dotted lines: without D^p_{ij}.

importance of the term $\varepsilon^h_{ij}\partial U_i/\partial x_j$ in equation (3.3): as shown in figures 6, 7 and 8, the conventional form of the model $P^1_\varepsilon + P^2_\varepsilon = 1.44\, P\varepsilon^h/k$ reproduces reasonably well the complete mixed production term (much better than when ε is used) and in the illustrations above (figures 16 to 19) we used this conventional expression. The slightly deficient wall imbalance of the $\overline{u_2u_2}$-equation affects only the asymptotic wall behaviour of $\overline{u_2u_2}$, but has a marginal effect on the other variables. This deficiency can be overcome by introducing, e.g., the 'pressure diffusion' correction of Launder & Tselepidakis (1993)†, as shown in figure 20.

5. Revision of the algebraic model for ε_{ij}

In § 2.1 we discussed the common expression for ε_{ij} and outlined the current practice in defining the 'blending' function f_s in terms of turbulence Reynolds number and invariants of the stress and dissipation rate anisotropy tensors. Good agreement with DNS data was demonstrated for diagonal components of ε_{ij}, but agreement was less satisfactory for the off-diagonal components (here ε_{12}). Since in the approach proposed here ε_{12} plays an important role in reproducing the production term P^1_ε close to a solid wall, an improvement in the modelling of ε_{ij} with a particular focus on off-diagonal components becomes more important. This is even more the case with other off-diagonal components in three-dimensional and non-equilibrium flows, such as in an axially rotating pipe, where ε_{23} combines with $\partial W/\partial r$ in the mixed production term.

Hanjalić & Launder (1976) argued that the blending function should account not only for the viscous effects and stress anisotropy, but also for the amount of mean shear felt by dissipative eddies during their lifetime. The argument was that the strain rate will impose a directional orientation on eddies of all sizes including the small-scale dissipative ones, particularly close to a solid wall where the eddy scales are generally small. The ratio of the dissipation (Kolmogorov) time scale $\tau_K = (\nu/\varepsilon)^{1/2}$ to

† The molecular diffusion and dissipation rate dominate the exact wall balance in the $\overline{u_2u_2}$-equation, when the conventional dissipation rate is used: $\mathscr{D}^p_{22} + \mathscr{D}^v_{22} - \varepsilon_{22} = -4\overline{c_2c_2}y^2 + 12\overline{c_2c_2}y^2 - 8\overline{c_2c_2}y^2 = 0$, and accounting for the pressure diffusion was not that important. This was the reason for neglecting pressure diffusion in the original HJ model. However, the influence of molecular diffusion and dissipation rate in the near-wall balance is reduced by factor 2 when using the 'homogeneous' stress dissipation rate, and accounting for the pressure diffusion becomes important.

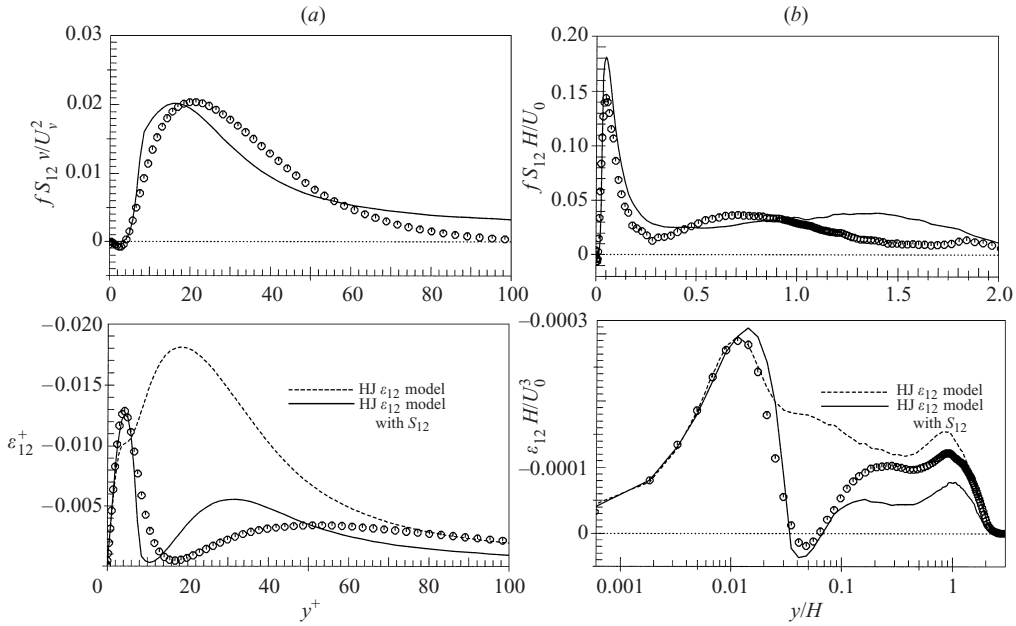

FIGURE 21. Profiles of the product fS_{12} and the off-diagonal dissipation correlation component ε_{12} obtained by the new model (equation (5.3)) in (*a*) the fully developed channel flow with symbols from DNS of Kim *et al.*, $Re_m = 13\,750$ and (*b*) in the recovery region of the flow over a backward-facing step with symbols from DNS of Le *et al.*, $Re_H = 5000$, $x/H = 15$.

the time taken by the mean strain to deform the small eddies, i.e. $\tau_K/\tau_S = (\nu/\varepsilon)^{1/2}S$ where $S = \sqrt{S_{ij}S_{ij}}$, was proposed as a convenient non-dimensional parameter to account for the strain effect. However, this idea was not pursued further because of the lack of information that could verify it.

Here we revisit the above idea by noting that the major deviation of *a priori* predictions of ε_{12} from DNS results occurs in the region where the strain rate effect on turbulence production is largest, i.e. around $y^+ \approx 20$ in channel flows, and in the shear layer behind a backward-facing step. In order to remedy this deficiency, we examined two possible modifications of expression (2.5) (consistent with the above introduction of the equation for the homogeneous dissipation rate ε^h). The first involves the multiplication of the function f_s by the scale ratio $\tau_K/\tau_S = \tau_K S$. While this seems attractive and feasible, the test did not show the desired effect: the shape of the off-diagonal stress dissipation rate ε_{12} was indeed improved, but the influence on the diagonal components was too strong. Further tuning could produce better results, but we turned to a different modification that implies the addition of an extra term to equation (2.14), so that the complete expression for ε_{ij}^h reads

$$\varepsilon_{ij}^h = \left[(1 - f_s)\tfrac{2}{3}\delta_{ij} + f_s \frac{\overline{u_i u_j}}{k} + 2f\, S_{ij}\tau_K \right] \varepsilon^h. \tag{5.1}$$

Taking the newly introduced function as

$$f = \min\left\{ AA_2, \left[1 - \exp\left(-\frac{Re_t}{150} \right) \right]^3 \right\} \tag{5.2}$$

yields a significant improvement in the reproduction of ε_{12} in a plane channel flow, as shown in figure 21.

It is noted that expression (5.1) follows from the proposal of Hanjalić & Launder (1980) mentioned earlier to enhance the effect of irrotational strain in the ε equation by adding the term $Cfk\Omega_{ij}\Omega_{ij}$. Combined with $P_\varepsilon^1 = \varepsilon_{ij}(\partial U_i/\partial x_j)$ (equation (3.2)), these two terms reduce for thin shear flows (for $\Omega_{ij} \approx S_{ij} \approx \frac{1}{2}\partial U_i/\partial x_j$) to

$$(\varepsilon_{ij} + Cf\tau S_{ij}\varepsilon)\frac{\partial U_i}{\partial x_j}. \tag{5.3}$$

Replacing ε_{ij} by expression (2.14) and τ by τ_K, applied to ε^h instead to ε, leads to expression (5.1).

The above proposal serves as an illustration of the necessity and possibility of accounting for the effect of mean rate of strain on ε_{ij}. Further work, with more extensive testing in a wider variety of flows, is needed before formulating a general and definite model.

6. Conclusions

The derivation of the dissipation equation from the two-point covariance and reformulation of the models of each term, using some novel arguments and the notions of the vorticity transport theory, shows that it is possible to perform term-by-term modelling for near-wall turbulent flows in good agreement with DNS data. Decisive advantages are achieved if the so-called homogenous dissipation $\varepsilon^h = \varepsilon - \frac{1}{2}\nu(\partial^2 k/\partial x_l \partial x_l)$ is considered, derived from the two-point velocity correlation equation. A consistent use of ε^h and the components of the stress dissipation rate tensor ε_{ij}^h in the complete model provides several benefits: it ensures satisfaction of wall limits without using any wall topography parameter, reduces the necessity for empirical inputs and enables better term-by-term reproduction of DNS data. The model ε^h equation in conjunction with a model stress equation, $\overline{u_i u_j}$, where dissipation is also expressed in terms of ε^h, constitute a new low-Reynolds-number second-moment closure model. Both *a priori* and full model computations of turbulent flows in a plane channel, constant-pressure boundary layer, behind a backward-facing step and in an axially rotating pipe, produced results for second-moment turbulence correlations and stress budget in good agreement with the available DNS results.

We thank Dr. J. R. Ristorcelli, (at present at Los Alamos National Laboratory) for his valuable contribution to the derivation of the model in § 3.2, while staying at Delft University of Technology as a J. M. Burgers Centre visiting researcher. We also acknowledge fruitful discussions with Dr J. Jovanović of the University of Erlangen.

Appendix. Low-Reynolds-number second-moment closure – $\overline{u_i u_j}$ – ε^h

(i) Reynolds-stress equation:

$$\frac{\mathrm{D}\overline{u_i u_j}}{\mathrm{D}t} = \frac{\partial}{\partial x_k}\left[\left(\tfrac{1}{2}\nu\delta_{kl} + C_s\frac{k}{\varepsilon^h}\overline{u_k u_l}\right)\frac{\partial \overline{u_i u_j}}{\partial x_l}\right] - \left(\overline{u_i u_k}\frac{\partial U_j}{\partial x_k} + \overline{u_j u_k}\frac{\partial U_i}{\partial x_k}\right) + \Phi_{ij} - \varepsilon_{ij}^h.$$

Pressure–strain model:

$$\Phi_{ij} = \Phi_{ij,1} + \Phi_{ij,1}^w + \Phi_{ij,2} + \Phi_{ij,2}^w,$$

$$\Phi_{ij,1} = -C_1\varepsilon^h a_{ij}, \quad \Phi_{ij,2} = -C_2\left(P_{ij} - \tfrac{2}{3}P_k\delta_{ij}\right),$$

$$\Phi_{ij,1}^w = C_1^w f_w \frac{\varepsilon^h}{k}\left(\overline{u_k u_m}n_k n_m\delta_{ij} - \tfrac{3}{2}\overline{u_i u_k}n_k n_j - \tfrac{3}{2}\overline{u_k u_j}n_k n_i\right),$$

$$\Phi_{ij,2}^w = C_2^w f_w\left(\Phi_{km,2}n_k n_m\delta_{ij} - \tfrac{3}{2}\Phi_{ik,2}n_k n_j - \tfrac{3}{2}\Phi_{kj,2}n_k n_i\right),$$

where

$$C_1 = C + \sqrt{A}E^2, \quad C = 2.5AF^{1/4}f, \quad F = \min\{0.6; A_2\},$$

$$f = \min\left\{\left(\frac{Re_t}{150}\right)^{3/2}; 1\right\}, \quad f_w = \min\left[\frac{k^{3/2}}{2.5\varepsilon^h x_n}; 1.4\right],$$

$$C_2 = 0.8A^{1/2}, \quad C_1^w = \max(1 - 0.7C; 0.3), \quad C_2^w = \min(A; 0.3).$$

Stress–dissipation rate model:

$$\varepsilon_{ij}^h = (1 - f_\epsilon)\tfrac{2}{3}\delta_{ij}\varepsilon^h + f_\varepsilon \frac{\overline{u_i u_j}}{k}\varepsilon^h, \quad \text{where} \quad f_s = 1 - \sqrt{A}E^2.$$

(ii) Dissipation equation:

$$\frac{\mathrm{D}\varepsilon^h}{\mathrm{D}t} = -C_{\varepsilon 1}\overline{u_i u_j}\frac{\partial U_i}{\partial x_j}\frac{\varepsilon^h}{k} - 2\nu\left(\frac{\partial \overline{u_i u_k}}{\partial x_l}\frac{\partial^2 U_i}{\partial x_k \partial x_l} + C_{\varepsilon 3}\frac{k}{\varepsilon^h}\frac{\partial \overline{u_k u_l}}{\partial x_j}\frac{\partial U_i}{\partial x_k}\frac{\partial^2 U_i}{\partial x_j \partial x_l}\right)$$
$$-C_{\varepsilon 2}f_\varepsilon\frac{\varepsilon^h\tilde{\varepsilon}^h}{k} + \frac{\partial}{\partial x_k}\left[\left(\tfrac{1}{2}\nu\delta_{kl} + C_\varepsilon\frac{\varepsilon^h}{k}\overline{u_k u_l}\right)\frac{\partial \varepsilon_h}{\partial x_l}\right].$$

Summary of the remaining coefficients: $C_s = 0.22, C_\varepsilon = 0.18, C_{\varepsilon 1} = 1.44, C_{\varepsilon 2} = 1.80, C_{\varepsilon 3} = 0.32, f_\varepsilon = f_\varepsilon = 1 - (C_{\varepsilon 2} - 1.4)/C_{\varepsilon 2}\exp[-(Re_t/6)^2]$.

REFERENCES

Bernard, P. S. 1990 Turbulent vorticity transport in three dimensions. *Theor. Comput. Fluid Dyn.* **2**, 165–183.

Bradshaw, P., Launder, B. E. & Lumley, J. L. 1991 Collaborative testing of turbulence models. *Trans. ASME: J. Fluids Engng* **113**, 3–4.

Bradshaw, P. & Perot, J. B. 1993 A note on turbulent energy dissipation in the viscous wall region. *Phys. Fluids* A **5**, 3305–3306.

Coleman, G. N. & Mansour, N. N. 1993 Simulation and modelling of homogeneous compressible turbulence under isotropic mean compression. In *Turbulent Shear Flows* (ed. F. Durst *et al.*), vol. 8, pp. 269–282. Springer.

Craft, T. J. & Launder, B. E. 1996 A Reynolds stress closure designated for complex geometries. *Intl J. Heat Fluid Flow* **17**, 245–254.

Daly, B. J. & Harlow, F. H. 1970 Transport equations in turbulence. *Phys. Fluids* **13**, 2634–2649.

Durbin, P. A. 1991 Near-wall turbulence closure modeling without 'damping functions'. *Theor. Comput. Fluid Dyn.* **3**, 1–13.

Durbin, P. A. & Speziale, C. G. 1991 Local anisotropy in strained turbulence at high Reynolds numbers. *Trans. ASME: J. Fluid Engng* **117**, 707–709.

Eggels, J. G. M., Boersma, B. J. & Nieuwstadt, F. T. M. 1994 Direct and large-eddy simulations of turbulent flow in an axially rotating pipe. *Int. Rep.* Lab. for Aero- and Hydrodynamics, Delft University of Technology, Delft, The Netherlands.

Gilbert, N. & Kleiser, L. 1991 Turbulence model testing with the aid of direct numerical simulation results. In *8th Symp. on Turbulent Shear Flows, TU Munchen*, p. 29.1.

Hallbäck, M., Groth, J. & Johansson, A. V. 1990 An algebraic model for nonisotropic turbulent dissipation rate in Reynolds stress closures. *Phys. Fluids* A **2**, 1859–1866.

Hanjalić, K. & Jakirlić, S. 1993 A model of stress dissipation in second-moment closures. *Appl. Sci. Res.* **51**, 513–518.

Hanjalić, K. & Jakirlić, S. 1998 Contribution towards the second-moment closure modelling of separating turbulent flows. *Computers Fluids* **27**, 137–156.

Hanjalić, K. & Launder, B. E. 1972 A Reynolds stress model of turbulence and its application to thin shear flows. *J. Fluid Mech.* **52**, 609–638.

Hanjalić, K. & Launder, B. E. 1976 Contribution towards a Reynolds-stress closure for low Reynolds number turbulence. *J. Fluid Mech.* **74**, 593–610.

Hanjalić, K. & Launder, B. E. 1980 Sensitizing the dissipation equation to irrotational strains. *Trans. ASME: J. Fluids Engng* **102**, 34–40.

Jakirlić, S. 1997 Reynolds-Spannungsmodellierung komplexer turbulenter Strömungen. PhD Thesis, Erlangen-Nuremberg University.

Jakirlić, S. & Hanjalić, K. 1995 A second-moment closure for non-equilibrium and separating high- and low-Re-number flows. In *Proc. 10th Symp. on Turbulent Shear Flows, The Pennsylvania State University, University Park, PA*, vol. 3, pp. 23.25–23.30.

Jovanović, J., Ye, Q.-Y. & Durst, F. 1995 Statistical interpretation of the turbulent dissipation rate in wall-bounded flows. *J. Fluid Mech.* **293**, 321–347.

Kawamura, H. & Kawashima, N. 1995 A proposal of k–$\tilde{\varepsilon}$ model with relevance to the near-wall turbulence. In *Turbulence, Heat and Mass Transfer* (ed. K. Hanjalić & J.C.F. Pereira), vol. 1, pp. 197–202. Begell House.

Kebede, W., Launder, B. E. & Younis, B. A. 1985 Large-amplitude periodic pipe flow: a Second-Moment Closure study. In *5th Symp. on Turbulent Shear Flows, Cornell University, Ithaca, New York*, p. 16.23.1.

Kim, J., Moin, P. & Moser, R. 1987 Turbulence statistics in fully developed channel flow at the low Reynolds number. *J. Fluid Mech.* **177**, 133–166.

Launder, B. E. & Reynolds, W. C. 1983 Asymptotic near-wall stress-dissipation rates in a turbulent flow. *Phys. Fluids* **26**, 1157.

Launder, B. E. & Tselepidakis, D. P. 1993 Progress and paradoxes in modelling near-wall turbulence. In *Turbulent Shear Flows* (ed. F. Durst *et al.*), vol. 8, pp. 81–96. Springer.

Lee, M. J. & Reynolds, W. C. 1987 On the structure of homogeneous turbulence. In *Turbulent Shear Flows* (ed. F. Durst *et al.*), vol. 5, pp. 54–66. Springer.

Mansour, N. N., Kim, J. & Moin, P. 1988 Reynolds stress and dissipation-rate budgets in a turbulent channel flow. *J. Fluid Mech.* **194**, 15–44.

Nagano, Y. & Shimada, M. 1993 Modelling the dissipation-rate equation for two-equation turbulence model. In *Proc. 9th Symp. on Turbulent Shear Flows, Kyoto*, p. 23.2.1.

Oberlack, M. 1997 Non-isotropic dissipation in non-homogeneous turbulence. *J. Fluid Mech.* **350**, 351–374.

Orlandi, P. & Ebstein, D. 2000 Turbulent budgets in rotating pipe by DNS. *Intl J. Heat Fluid Flow* **21**, 499–505.

Rodi, W. & Mansour, N. N. 1993 Low Reynolds number $k-\varepsilon$ modelling with the aid of direct numerical simulation data. *J. Fluid Mech.* **250**, 509–529.

Rubinstein, R. & Zhou, Y. 1997 The dissipation rate transport equation and Subgrid-Scale Models in rotating turbulence. *NASA/CR*-97-206250; *ICASE Rep.* 97-63.

Spalart, P. R. 1988 Direct simulation of a turbulent boundary layer up to $R_\theta = 1410$. *J. Fluid Mech.* **187**, 61–98.

Speziale, C. G. & Gatski, T. B. 1997 Analysis and modelling of anisotropies in the dissipation rate of turbulence. *J. Fluid Mech.* **344**, 155–180.

Tagawa, M., Nagano, Y. & Tsuji, T. 1991 Turbulence model for the dissipation rate of turbulence. In *Proc. 8th Symp. on Turbulent Shear Flows, Munich, Germany*, p. 29.3.1.